CREATING MULTI-TOUCH HAPTIC FEEDBACK ON AN ELECTROSTATIC TACTILE DISPLAY

by

Gholamreza Ilkhani Sarkandi

B.S., Mechanical Engineering, Azad University of Tabriz, 2006

M.S., Mechatronics Engineering, Sharif University of Technology, 2010

Submitted to the Institute for Graduate Studies in
Science and Engineering in partial fulfillment of
the requirements for the degree of
Doctor of Philosophy

Graduate Program in Mechanical Engineering

Boğaziçi University

2017

ACKNOWLEDGEMENTS

At the risk of missing somebody...

First, I would like to thank my adviser, Professor Samur for his encouragement and support over the last five years. I have been extremely lucky to work with him. I hope to one day to follow in his footsteps and become an academic man like him.

I gratefully acknowledge Prof. Cetin Yilmaz and Prof. Senol Mutlu for their constructive and priceless advice during my graduate study. Also I would like to thank Prof. Cagatay Basdogan and Prof. Yildiz who accepted to be in my jury committee despite their tight schedule.

I would like to thank all the members of Haptics and Robotics laboratory have come and gone over the years. They provided me friendship, diversions and useful ideas. Two of my long time friends Ramin and Alireza who always helped with the thesis.

The research presented in this thesis was supported by a grant from the Scientific & Technological Research Council of Turkey (TUBITAK) project number 113E601.

I thank most highly my family especially my father and mother to whom I dedicate this thesis. There are not enough words I can say to describe you.

Finally, to God be all the glory...

ABSTRACT

CREATING MULTI-TOUCH HAPTIC FEEDBACK ON AN ELECTROSTATIC TACTILE DISPLAY

This study is composed of two main parts. In the first part, we present single touch electrostatic tactile display analysis and modelling together with some preliminary observation on conventional rendering methods. Data-driven texture rendering method is introduced and examined in two steps. First, accelerations occurring due to sliding a tool on three different surfaces are measured, and then the collected data are replayed on an electrostatic tactile display. Second, data from the Penn Haptic Texture Toolkit (HaTT) are used to generate virtual textures on the same tactile display. Psychophysical experiments are carried out for both steps. The results show that the virtual textures generated using the data-driven method are mostly similar to the real textures in comparison to conventional method of rendering. Together with the supporting results from the multidimensional scaling (MDS) analysis, it is shown that the data-driven method is a viable solution for realistic texture rendering. In the second part, we propose a method and present a tactile display prototype to create multi-touch haptic feedback using electrostatic attraction. The method relies on applying high-voltage AC signals on certain orthogonal electrode lines resulting in perceivable changes of friction at the intersection points. Generated surface friction on the prototype is measured with a planar tribometer. Results show that multiple localized friction spots can be generated with the proposed method. A user study is also performed to test the prototype in a multi-touch scenario where a virtual texture is explored by two fingers simultaneously. Quantitative and qualitative analyses demonstrate the feasibility of creating multi-touch haptic feedback on an electrostatic tactile display.

ÖZET

ELEKTROSTATIK BIR DOKUNMATIK EKRANDA ÇOKLU DOKUNSAL GERIBESLEME OLUŞTURULMASI

Bu çalışma iki ana kısımdan oluşmaktadır. İlk kısımda tek dokunmalı elektrostatik dokunsal ekran analiz ve modellemesi ön gözlemler ve geleneksel görüntü oluşturma yöntemleriyle birlikte sunulmuştur. Veri bazlı doku görüntü oluşturma yöntemi gösterilmiş ve iki adımda incelenmiştir. İlk olarak bir ucun 3 farklı yüzeyde kayması sonucu oluşan ivmeler ölçülmüş ve sonrasında toplanan veri elektrostatik dokunsal bir yüzeyde tekrar oynatılmıştır. İkinci olarak aynı dokunsal yüzeyde sanal dokular oluşturmak için Penn Haptic Texture Toolkit'ten (HaTT) gelen veri kullanılmıştır. Psikofiziksel deneyler iki adımda gerçekleştirilmiştir. Sonuçlar veri bazlı yöntemle oluşturulan sanal yüzeylerin gerçek dokulara benzer olduğunu göstermiştir. Çok boyutlu ölçeklendirme analizinden alınan destekleyici sonuçlarla birlikte veri bazlı yöntemin gerçekçi doku görüntüsü oluşturmada uygulanabilir bir çözüm olduğu ortaya konmuştur. İkinci kısımda bir yöntem önerilmiş ve elektrostatik çekim kullanarak çok dokunmalı haptik geribildirim oluşturan dokunsal ekran prototipi sunulmuştur. Yöntem belirli ortogonal elektrot hatlarına yüksek gerilimli AC sinyali uygulanmasıyla kesişim noktalarında algılanabilir sürtünme değişikliği oluşturulmasına dayanmaktadır. Prototipte oluşturulan yüzey sürtünmesi düzlemsel tribometr ile ölçülmüştür. Sonuçlar birden fazla bölgesel sürtünme noktaları oluşturulabildiğini göstermiştir. Prototipi sanal bir yüzeyin iki parmakla keşfedildiği çok dokunmalı bir senaryoda denemek amacıyla kullanıcı deneyleri yapılmıştır. Nicel ve nitel analizler çok dokunmalı haptik geribildirimin elektrostatik dokunsal ekranda oluşturmanın uygulanabilirliğini ortaya koymuştur.

TABLE OF CONTENTS

LIST OF FIGURES

LIST OF SYMBOLS

A	Contact area
a_k	Autoregressive model coefficients
C	Total capacitance
c_k	Moving average model coefficients
C_r	Capacitance across the insulator layer
C_s	Capacitance across the stratum corneum
D	Data-driven signal
d	Euclidean distance
dB	Decibel
F	Electrostatic force in parallel plate capacitor
F_0	Surface friction when all stimuli are OFF
F_B	Boundary electrostatic force
F_E	Electrostatic attractive force
F_{E1}	Electrostatic force across insulator layer
F_{E2}	Electrostatic force across stratum corneum
F_L	Dynamic friction
F_N	Normal force
G	Gravity
M	Mean
p	Autoregressive model order
q	Moving average model order
Q	Total charge
S	Square wave
S_p	Maximum peak spacing
T_1	Thickness of insulator layer above Y elecrode line
T_3	Thickness of insulator layer above X elecrode line
T_r	Thickness of the insulator layer
T_s	Thickness of the skin (stratum corneum)

V	Voltage
V_r	Voltage across insulator layer
V_s	Voltage across stratum corneum
Vpp	Peak to peak voltage
X	Axis in a coordinate system
Y	Axis in a coordinate system
ε_0	Permittivity of vacuum
ε_r	Dielectric constant of the insulator layer
ε_s	Dielectric constant of the skin (stratum corneum)
μ	Coefficient of dynamic friction
μ_s	Coefficient of static friction

LIST OF ACRONYMS/ABBREVIATIONS

2D	Two dimensional
3D	Three dimensional
ABS	Acrylonitrile butadiene styrene
AC	Alternating current
Al	Aluminium
ANOVA	Analysis of variance
AR	Autoregressive
ARMA	Autoregressive–moving average
D/A	Digital to analogue converter
DAQ	Data acquisition
DC	Direct current
ERM	Eccentric rotating mass
EV-Pen	Electrovibration pen
GUI	Graphical user interface
HaTT	Penn haptic texture toolkit
HF	Hydrofluoric acid
IR	Infrared
ITO	Indium tin oxide
LRA	Linear resonant actuator
MA	Moving average
MDS	Multidimensional scaling
MRF	Magnetorehological fluid
NI	National instrument
OCA	Optically clear adhesive
P-Cap	Projected capacitive
PR	Photoresist
PVDF	Polyvinylidene difluoride
RF	Radio frequency

SD	Standard deviation
TPaD	Tactile pattern display
UV	Ultraviolet
wgn	White Gaussian noise

1. INTRODUCTION

Tactile feedback is a significant factor while interacting with electronic devices in which human-machine interaction is important. It transforms an electronic device to a bilateral one which gets an input, and outputs a sensational awareness [1]. This sensational awareness arising from exchange of information between the body and the outside world while touching an object is called *haptics* [2]. Haptic technology is the science of generating sense of virtual touch by implying different phenomena such as vibration, shear force and temperature [3]. Despite the various possibilities in haptic technology, a proper method must be adopted to create an intuitive haptic feedback and to complete the bilateral cycle between human and machine, specially in touch screen devices.

1.1. Motivation

Utilizing haptic feedback enhances device usability and increases realism by enabling combination of touch, vision and sound. Unlike characteristic of input to touch screen devices, in the absence of tactile information the output is struggling to present itself in the best way and is hard to accomplish. Most of the touch screen devices do not provide tactile feedback and relies only on audio-visual feedback to convey information. Smart phones, computers, and tablets do not exploit the full capacity of this technology, and are limited to vibrational applications. Consequently, the effort to advance operative, practical and inexpensive tactile feedback for the touch screen interface has increased [4].

Designing user-friendly touch interfaces is challenging. Touch screen devices are just equipped with primitive form of tactile feedback and can just provide poor tactile information. In this sense, the most common feedback technique used in touch screen devices is using commercially available low-frequency vibration components such as eccentric rotating mass (ERM), linear resonant actuator (LRA) and piezo actuators [5]. Figure 1.1 shows an example of this technology used in mobile phones. These

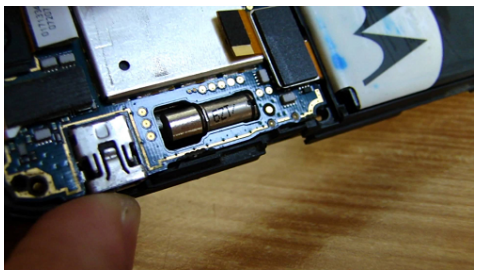

Figure 1.1. Low-frequency vibration is created by commercially available components such as ERM [6].

technologies do not satisfy customer demands for a sophisticated tactile interface to be engaged and immersed in the virtual world. For this reason, additional controls (e.g Fling joystick for ipad) have been added to touch screen devices to remove this gap.

Different technologies have been proposed by the researchers to create a sense of touch. For instance electrostimulation (Electrocutaneous), acoustic wave, magnetorehological fluids (MRF) and, shape memory alloy [7–10] are among the favorable methods of creating tactile feedback. Despite the interaction opportunities which these technologies provide, still feasible and lightweight displays are absent. Mechanical solutions [11–13] are impractical and are not adaptable in current touch display system. The electrocutaneous method is not favorable because of the small current passing through the finger which sometimes gives an unpleasant feeling to user. [14]. As a result, most of the tactile displays built to this day miscarry meaningful tactile information, are not practical and, they are restricted to small number of actuators with low-spatial density. For the reasons stated above, tactile displays have seldom made it to the commercial market.

In recent years, controlling friction force between finger and surface were proposed as a new technique for tactile feedback. If the friction force changes when the finger moves laterally, geometric and material properties of a virtual object can be presented to the user. This method also called *surface haptics*, modulates friction force to create texture perception. There are two methods proposed in the literature to change

lateral forces; *ultrasonic vibration* and *electrovibration*. Ultrasonic method is good at controlling friction force on a surface, however it is difficult to obtain this phenomenon in larger displays and achieve multipoint variable friction force. The second method is the method of electrovibration, which relies on creating an electrostatic force between finger and display [15–17]. Although this method is applicable to the current display systems, it faces some shortcomings. Electrovibration method is limited to single touch systems currently. This means that friction force is distributed on surface uniformly and equally. In other words, all the fingers feel the same force. However, the localization of feedback is required to benefit from the rapidly growing multi-touch systems (Figure 1.2).

Besides showing the feasibility of creating touch feedback using electrostatics, a few studies emphasized on rendering and evaluating techniques for generating rich tactile feedback [18]. *Data-driven* or measurement-based haptic rendering is an emerging technique providing an opportunity to record data from real objects and replay them on a system [19, 20]. The realism provided is the primary advantage of using measurement-based haptic modeling [21], therefore we can simplify rendering of real materials in virtual space without explicit knowledge about or setting of material properties. Data-driven method could be an alternative for the current method of rendering which relies on trial and error.

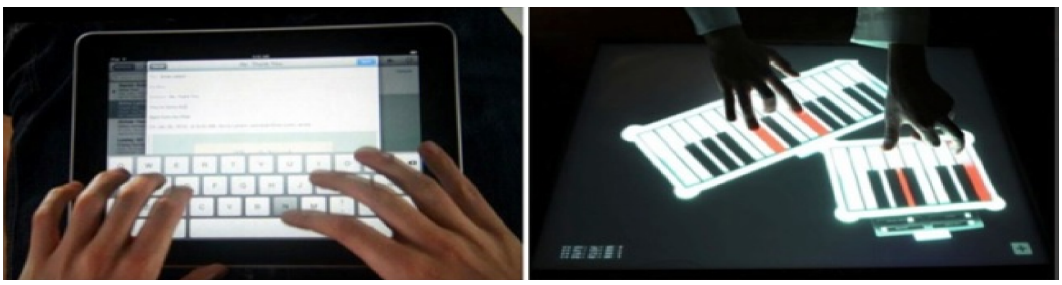

Figure 1.2. Multi-touch interaction with a virtual environment using both hands. Haptic feedback can increase accuracy, realism and immersion in the virtual space [6].

1.2. Objectives

The target area of this research is all types of touch screen systems such as smartphones and tablets, in which tactile feedback is necessary. By doing this research, we expect to reach the following objectives, to solve the problems discussed in the previous sub-chapter:

(i) Development and characterization of a single-touch electrostatic tactile display.
(ii) Development and evaluation of a data-driven texture rendering method for realistic virtual textures.
(iii) Developing of a multi-touch electrostatic tactile display.
(iv) Evaluation of feedback capacity of the developed multi-touch electrostatic tactile display.

1.3. Contributions

This work focuses on creating richer stimulation on electrostatic tactile display. First, an innovative texture rendering method is introduced to create perceptual illusion of touching a real material on a tactile display. This method provides a solution to one of the major problems related to texture rendering on electrostatic tactile display. Second, a novel tactile display is developed and fabricated. The proposed display provides independent stimuli to multiple fingers, realizing multi-touch haptic.

1.4. Outline

This thesis is organized in the following way. After this introductory chapter, first, texture perception is reviewed in real and virtual environments in Chapter 2. Necessary dimension for tactile perception and different modes of exploration are described. Roughness and its categorization in terms of surface irregularities are explained. In addition, the state-of-the-art surface haptic devices are surveyed. Next focus of the literature survey is on single and multi-touch sensors for touch detection with brief descriptions of their operating principles. Finally, data-driven texture rendering methods

are reviewed.

In Chapter 3, the single touch electrostatic tactile display is introduced. Induced electrostatic force on the finger tip is modelled and calculated. Analyses are performed to understand the operating principle of the display. At the end of this section, feasibility of using data-driven signals for surface rendering is investigated. The proposed data-driven method is evaluated in two complementary studies.

Chapter 4 is dedicated to the multi-touch electrostatic tactile display. Fabrication methods followed to develop the display in different configurations are explained step by step. Furthermore, quantitative and qualitative experiments to measure friction variation on the developed display for single and multiple points stimulation are presented.

Finally, the outcomes and contributions of this thesis are summarized in Chapter 5. Besides, possible future research directions are discussed in this chapter.

2. LITERATURE SURVEY

When we touch an object, haptic signals are sent to brain. Texture information is obtained through tactile receptors and kinesthetic sensation. In touch screen devices the kinesthetic information is absent and touch signals are limited to tactile information. This makes rendering issue very difficult since part of information which helps brain to interpret touch signals does not exist. However, current technologies allow us to create virtual texture mimicking the experience of touching a real object. In this section, texture and its properties are defined. Qualities or dimensions which help us to identify textures are discussed. The state-of-the-art tactile displays, with focus on surface haptics are investigated. Finally, haptic rendering methods are presented.

2.1. Texture Perception

Texture by definition is the shape of a surface or substance. In haptics literature, texture represents the qualities of a surface that body perceives while touching of an object. These qualities can be smoothness, roughness, softness, etc. of object. In fact, these qualities (perceptual dimensions of tactile textures) are the descriptors which are used to perceive surface properties. At least two dimensions are necessary for tactile texture perception and maximum number of these dimensions must be covered for a realistic haptic rendering [22]. The qualities are extracted using psychophysical evaluation methods. A detailed description of psychophysical methods can be found in [23,24]. Yoshida *et al.* [25] extracted four dimensions through multidimentional scaling analysis among 25 different materials. The results showed clear opposition between fibers and metals. Later Shirado & Maeno [26] considered four factors: *Roughness*, *Coldness*, *Moisture* and *Hardness* to relate object surface physical properties and texture perception through multivariate analysis. Guest *et al.* [27] conducted a series of experiments for developing a lexicon for touch. Their study showed that 262 adjectives were employed to express the sense of touch. Okamoto *et al.* [28] summarized dimensions for texture perception and identification as 1) rough/smooth, 2) hard/soft, 3) sticky/slippery, and 4) warm/cold (see Figure 2.1). Among all, roughness is the most

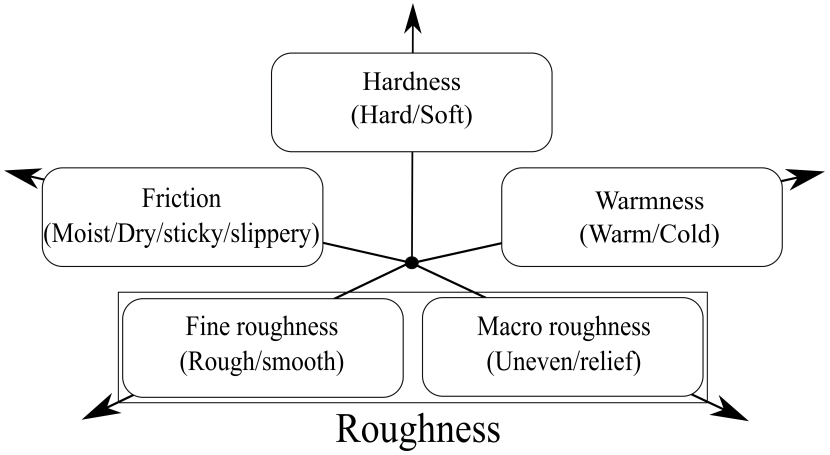

Figure 2.1. Psychophysical dimensions of tactile perception for material/texture [28].

important quality in texture perception [29].

Roughness perception is cutaneous [30]. However, it does not show the same behavior in different touch modes [22]. The modes could be summarized as *direct* (finger is in contact with the surface), *indirect* (surface scanned with a handheld probe), *passive* (only tactile cues are presented to a stationary finger contacting a surface that may or may not be moving), *active* (subject moves his/her finger over a stationary surface), and *pseudo-passive* (experimenter moves the subject's hand across a stationary surface) [30–32]. In [33], Klatzky & Lederman evaluated the feeling of roughness in direct and indirect modes. They showed that vibratory cues were dominant when a rigid link is used to perceive roughness, whereas both vibratory and spatial cues were utilized when the surface was explored with a bare finger. Their study suggests the viability of vibration in roughness augmentation [34]. Lederman *et al.* [35] also investigated influence of speed in indirect active and passive modes. Speed showed larger effect in passive exploration. Texture perception in direct and indirect modes were reviewed by Yoshika *et al.* [36] too. They showed that the arrangement of textures in a perceptual space based on judgments of roughness was similar in probe-scanning and finger-scanning conditions. They attributed roughness to vibration, texture compliance to hardness, and stickiness to friction. Stickiness or friction represents how much a finger adheres to the surface and roughness is related to the size of surface irregularities

or surface coarseness. Roughness can be divided in two groups according to pitch size of surface irregularities. The pitch size greater than ~ 200 μm is called *macrostructure*, and smaller ones are called *microstructure* [37]. Perception of microstructure surface happens in a different way than macrostructure surface. Very fine textures are perceived through vibration, whereas coarse surfaces are perceived through pressure [38]. In general, roughness, is hard to discuss directly from the physics of an object. Therefore, a productive approach must be taken for surface modelling through roughness representation.

2.2. Surface Haptics

Surface haptics is the study of artificially creating tactile perception when a fingertip and a surface are in physical interaction [39]. Surface haptics relies on modulating friction force between the finger and the surface. Friction modulation in touch interfaces improves physicality of the touched surface. Ultrasonic vibration [40–42] and electrostatic attraction [15, 43–45] are among the most popular methods for friction modulation. In the coming parts, state-of-the-art technologies employed for friction modulation, and hence for texture rendering are introduced.

2.2.1. Ultrasonic Method

One of the strong candidates to create haptic feedback is to use transverse ultrasonic vibrations on a tactile display. Unlike the electrostatic method which increases surface friction force, friction is reduced in ultrasonic vibration. Piezoelectric actuators are glued to peripheral of a glass plate, and are used to excite the plate at its resonant frequency [46]. Finger experiences lower friction force as vibration amplitude increases. The first ultrasonic vibrating plate was developed by Watanabe and Fukui [47] as is seen in Figure 2.2. In their device the resonance frequency was 76 kHz. An air film between a bar and a bare finger was created by vibrating the bar at this frequency. Later, Biet *et al.* [48] used this method on a metallic sheet. They glued an array of piezoelectric actuators to the underside of a metallic sheet. Ultrasonic vibration of the actuators put the sheet in a resonance, and created a squeeze film between the bare finger and

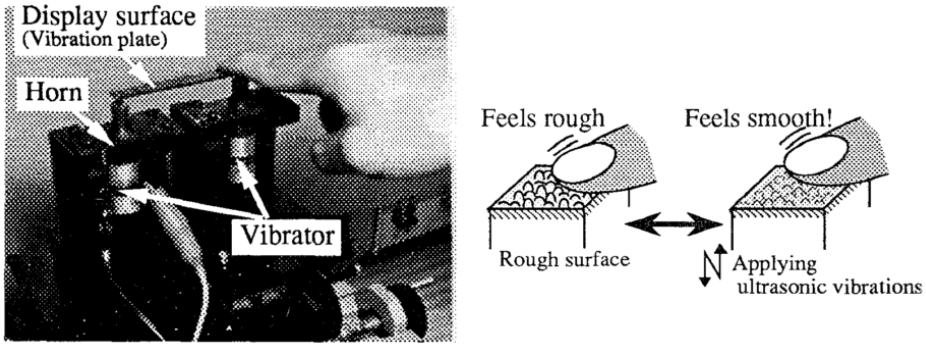

Figure 2.2. Experimental apparatus used by Watanabe and Fukui to create ultrasonic vibration. Vibrating the bar at 76 kHz creates a squeeze film which results in decrease in friction force [47].

the metalic plate. The Tactile Pattern Display (TPaD) [49–51], ShiverPad [52], LateralPad [53], ActivePaD [54] are series of studies which employed ultrasonic vibration to create different texture patterns. Figure 2.3 shows the LateralPad capable of creating vibratory motion in two directions using piezo actuators. Kim *et al.* [55] showed how amplitude-modulated signal can be used to create simple sinusoidal patterns. They performed a user study to identify the relationship between input signal parameters and a rendered texture output. The experimental results provide a relationship between a driving voltage amplitude and the depth (or equivalently the amplitude) of the rendered roughness as well as a relationship between the input signal frequency and the wavelength (or equivalently the wave number) of output tactile sensation.

There are two theories explaining the ultrasonic vibration method. The first hypothesis relies on the contribution of air to ultrasonic friction reduction. This idea explains that when a finger is set on a plate which is vibrating with a resonant frequency, a squeeze air film is formed between the finger and the surface. If the high pressure in this film overcomes the normal force applied by the finger, then the finger float on a cushion of air. This idea was addressed by Ben Messaoud *et al.* [56] where friction between a sliding finger and a device was recorded for an ambient pressure of 0.5 and 1 atm. The plate vibrational amplitude was set between 0.5 and 2 μm with an increment of 0.5 μm. The results showed that ambient pressure (squeeze film) is responsible for

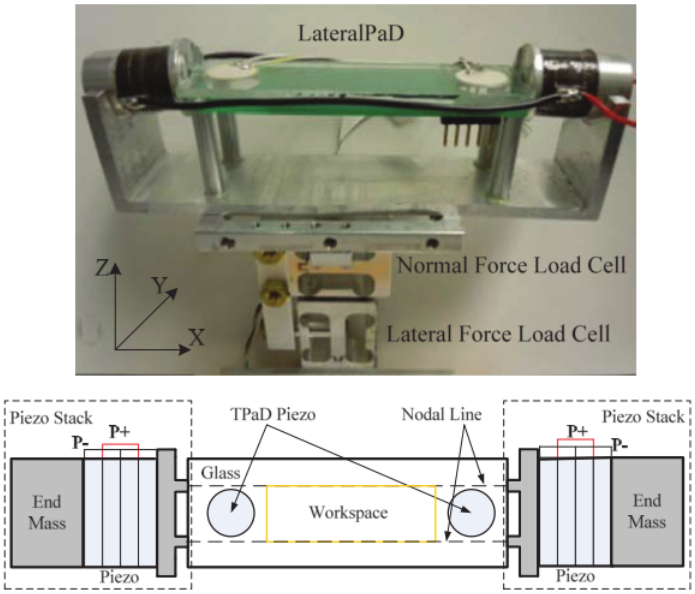

Figure 2.3. LateralPad is capable of creating out of plane motion and lateral vibration. Shear force is developed in the light yellow rectangular region where significant shear force can be developed [53].

the 40 percent of the friction reduction. Recently a similar investigation was performed by Friesen *et al.* [57]. An artificial finger is used instead of a real one in contact with an ultrasonic tactile display inside a vacuum chamber. Friction between the finger and the glass was measured by rotating the finger with a motor and changing pressure of the chamber. The motor's torque load was measured as an indicator of change of friction force. Decreased friction is signaled by decreased motor current. The study shows contribution of the air in friction reduction. The second theory on the ultrasonic vibration method considers the effect of intermittent contact of the finger. Wiertlewski *et al.* [58] developed a high resolution optical sensor to observe true area of contact between the finger tip and a glass surface. The measurements reveal that an increase in vibration amplitude leads to a clear reduction of the true area of contact and the interfacial friction.

The ultrasonic method was also extended to multi-touch applications. Ghenna *et al.* [59] suggested a method to control ultrasonic waves on a beam, allowing to obtain a multi-touch ultrasonic tactile stimulation on two points. The same authors presented an extension of this method in two dimensions. They glued piezoelectric actuators to four corners of the plate. Piezo actuators caused vibration of the plate in and out of plane mode in two directions (say X and Y directions). The vibration control of X mode according to Y one allows to smooth and continuous change of position of nodes and antinodes [60]. Consequently if friction force in nodes is minimum, it is maximum in antinode points. This enabled them to control friction force under each finger. Although the ultrasonic method is a good choice for haptic rendering on touch screens, it is hard to achieve friction control in larger displays and the obtained result is noisy [61]. It is also hard to achieve multi-touch application in which force level is not limited to minimum and maximum. Rendering complex textures is harder in this method too, since transition from low friction to high friction is slow [62].

2.2.2. Electrovibration Method

In this method, small electrostatic forces are generated between a finger and a surface consisting of a conductor covered with a thin insulating layer. This phenomenon based on electrostatic attraction, also called *electrovibration* [63, 64], has recently become the favored method to generate tactile feedback on touchscreens [18, 65]. Although this technology was first adapted by Senseg to create haptic feedback in mobile phones [44], *TeslaTouch* is the most famous one which was introduced in 2010 [15]. In this method, when an alternating voltage is applied to the conductor, the capacitive layer between the finger and the conductor is charged, creating an electrostatic attraction that increases surface friction. This alteration modulates lateral friction force and creates a vibration on the finger pad as finger is moved across the surface. Distinct sensations, such as roughness, can be produced by altering the input voltage (see Figure 2.4). Periodic signals such as sinusoidal or square waves are used for this purpose. These signals are tuned by varying amplitude and frequency to model different textures [39, 66].

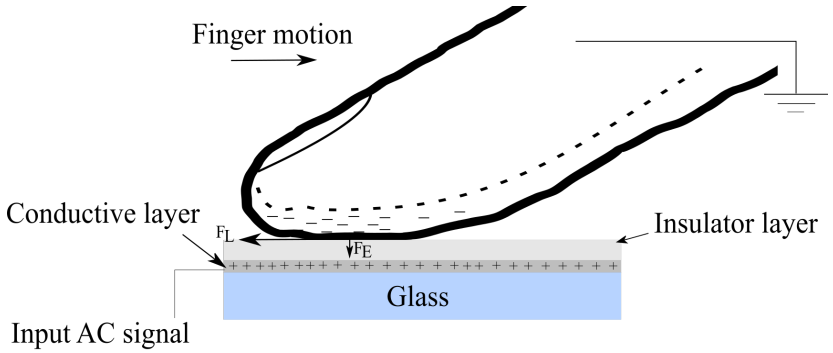

Figure 2.4. AC signal is applied to a conductive surface. Periodic attractive force between a sliding finger and the panel is created (F_E). Thus, a dynamic friction force (F_L) is created between the finger and the display.

Israr *et al.* [67] introduced a mobile, generic, and inexpensive visuo-tactile sensory substitution device for the visually impaired. The proposed assistive device consists of a surface capacitive touch-panel, a camera attached on the back, and hardware driver. The device helps users to explore the world around them, by pointing it towards objects of the environment and rendering tactile information to the objects sensed by a camera (Figure 2.5). In a similar study by Xu *et al.* [68], TeslaTouch was used to provide tactile sensation to visually impaired people to interpret and create 2D tactile information such as dots to map braille letters to tactile sensation (Figure 2.5). Osgouei *et al.* [69] extended 2D tactile information to 3D primitive geometrical shapes using electostatically created patterns. Authors doubted capability of electrovibration method for 3D rendering. Heewon *et al.* [70] studied the effect of environmental parameters on electrovibration feedback generation. They introduced a method to compensate nonuniform perceived intensity due to varying environmental impedance. In [71–73], Wu *et al.* introduced a method for rendering a virtually created surface based on the image quality. Using image properties, they modulated input signal amplitude and frequency. Since these parameters are important in friction modulation Vardar *et al.* [74], recently investigated the effect of input voltage waveform on haptic perception of electrovibration on touch screens. According to their observation, subjects are most sensitive to square wave signals than sinusoidal ones for frequencies lower than 60 Hz. Kaczmarek *et al.* [75] studied polarity effect of the pulsed excitation on electrovibratory

perceptual sensitivity. They concluded that a waveform with negative polarity shows stronger perceptual sensitivity than positive pulses. For low voltage operation, Kang *et al.* [76,77] investigated effects of input voltage signals on the perceived intensity of electrovibration. Among three types of signals, they conclude that the DC-offset method is the best way to lower the driving voltage amplitude while providing perceptually equivalent electrovibrations.

(a) (b)

Figure 2.5. a) A visually impaired person explores the surrounding using an electrostatic tactile display [67]. b) A person explores the electrostatic tactile display to interpret 2D patterns such as circles [68].

In some studies, electrovibration method is combined with multiple haptics technologies. These studies known as Cross-Field Haptics [78] aim to solve the problem associated with the electrovibration method in which relative motion between finger and surface is necessary to get a tactile feedback. Pyo *et al.* [79] introduced a haptic display that combines electrovibration with mechanical vibration. The developed system includes a PDMS layer between two conductive parallel plates. Stronger tactile information is created since mechanical vibration is combined with electrovibration. A similar study was done by Lee *et al.* [80] where PDMS layer was eliminated and an air gap was introduced between two plates. Giraud *et al.* [81, 82] combined an ultrasonic vibration with electrovibration to identify the effect of ultrasonic vibration on electrovibration stimulation. The measurements revealed that the squeeze film effect not only reduced the friction coefficient but also decreased the spikes produced by electrovibration.

Electrovibration method is not only used in direct mode but also is employed when the finger is not in direct contact with the surface. Wang *et al.* [83] introduced a hand-held device called Electrovibration Pen (EV-Pen) which incorporates electrovibration into pen interactions as is seen in Figure 2.6. The developed system not only has an advantage of pen-based interactions but also provides a wide range of haptic feedback modes without any form of mechanical actuator. Nakamura *et al.* [84–87] used multiple contact pads to render different frictional stimuli to different fingers. Each pad was controlled independently, therefore distinct texture patterns can be created under each pad (see Figure 2.6).

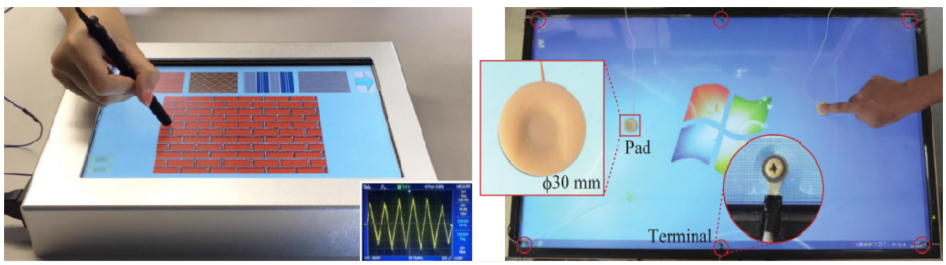

Figure 2.6. a) When the Ev-pen moves over a surface, an electrostatic force is created between the pen and the surface [83]. b) Contact pads are used to create electrostatic force [84].

Beside the electrovibration method, recently an electroadhesion method was introduced [88]. There is no fundamental difference between electrostatic and electroadhesion methods. Electroadhesion is a technique which creates higher attraction force [89]. It basically consists of an electrode, a dielectric and a cover insulator. Mullenbach *et al.* [90] developed a setup which provides opportunity to control the direction of the lateral force on a finger by electroadhesion method while the finger is in contact with an oscillatory surface. A similar study was conducted by Alma *et al.* [91] in which the experiments were performed on an electrostatic tactile display instead of electroadhesion tactile display. In his study, direction of lateral force was changed by synchronizing oscillatory motion and electrostatic force.

Studies which address electrovibration are limited to a single point haptic feedback. This means that the created feedback is the same and uniform at all points on the surface. Friction force (surface texture) can be varied from point to point if the finger position is measured, and the input signal is adjusted accordingly. This solution does not work if the surface is touched with more than one finger since there is only one conductive layer. This issue was addressed by Haga *et al.* [92]. They developed a new surface consisting of multiple rows and columns of electrodes in a matrix arrangement. Regional stimulation happens by selecting electrodes to be excited. They use beat phenomenon to create regional feedback. Although the study indicated that localized haptic feedback was possible with the proposed method, how it could be extended to multi-touch applications was not discussed. Another attempt to localize feedback on electrostatic display was done by Kim *et al.* [93]. The authors first claim that resistance of electrodes are important from the electrostatic tactile feedback point of view. Secondly, safety criteria on current was introduced. Although the stimulation method is not clear in this study, authors claim that by adding DC-offset they can lower the excitation voltage like in [76, 77]. The authors did not claim any intention to extend their method to reach multi-touch applications.

2.2.3. Miscellaneous Haptic Displays

2.2.3.1. Electrocutaneous Method. Electrocutaneous method was matter of interest among haptic community since 70's. It is known to be an effective way for transmitting visual and auditory information to the brain. Generally in this method a group of electrodes are developed [94]. When electrodes come in contact with the different part of the body such as forehead [95], finger tip [96–99], abdomen [100] and tongue [101] small amounts of electric current passes though the skin generating sensations of pressure or vibration and consequently illusion of object is created. Two main problems with this method are that: firstly, passed current gives an unpleasant feeling to the user and secondly, finger must consistently be in contact with electrode surface. Higashiyama *et al.* [102] studied how electrode location can alter elicited feeling from pleasant to painful. This method for hand held devices introduced by Altinsoy *et*

al. [103]. Study was performed in two parts. First, the relationship between current intensity, pulse frequency and roughness perception were investigated. Second, user study were performed for texture similarity perception while adjusting combination of parameters (intensity and frequency). Author concluded that high current intensity and low frequency pulses are mostly suitable for rough surface. On the contrary, low current intensity was suitable for smooth surface. Frequency had a neutral affect in second part.

Figure 2.7. 32×16 electrodes module for the forehead [95].

2.2.3.2. Lamb Wave Method. Lamb wave methods are mostly used to find finger position while finger is contact with a surface. This method utilizes time delay of an acoustic wave propagating in the plate [104, 105] to find a finger position [106]. Hudin *et al.* [107] used this method to create localized haptic feedback. Acoustic wave was created on a thin glass surface which was actuated by piezoelectric transducers located at the periphery. Inverse fourier transform of impulse responses between each pair of points and transducers was calculated for each transducer and each point of the surface. Then the time reversal operation consist on sending each actuator the time reversed signal corresponding to the actuation point was performed [108]. The result showed capability of the system for creating localized feedback.

2.2.3.3. Pin Array Tactile Display. Pin array display either developed for vibratory motion [109] to create a cutaneous sensation evoked by vibration or skin stretch to create embossing feeling under the finger [110]. Pasquero *et al.* constructed a tactile

display system known as STReSS capable of creating time-varying strain field at the skin surface. Using dense pin array, a programmable sequences of tactile images can be created by using this display [111].

2.3. Data-driven Rendering Method

Data-driven texture rendering is an emerging method for haptic rendering. In most data-driven haptic rendering studies, an intermediary tool captures data. The recorded data then played back on the same or other intermediary device by mechanical actuation. For instance, an interactive pen display was developed to capture and replay contact accelerations [112]. The study was complemented by Culbertson *et al.* [113] to account for the user's force and velocity. In both studies, acceleration signals were collected using an accelerometer, and voice coils attached to a pen were used as actuators. Figure 2.8 shows the pen shape device which is used for data collection and data playing. Pairwise comparisons between real and virtually created surface revealed good performance of the data-driven method in similarity ratings. Saga & Raskar [114] implemented a data-driven method on a touch display utilizing mechanical vibrations. They could create virtual textures and geometries on the touch display using both acceleration data directly recorded from the finger and gradual changes in lateral force. As is seen in Figure 2.8 an accelerometer is connected to the finger and captures occurred acceleration signal when finger explores surface of the material. Later collected signal is used in tactile display for rendering. Yamamoto *et al.* [115] used a PVDF (Polyvinylidene difluoride) sensor, a piezoelectric material that converts mechanical vibration into electrical signals, to record surface texture. The recorded electrical signals were used to render virtual textures on a tactile display consisting of a thin conductive film slider and stator electrodes. Psychophysical experiments performed with this system showed that subjects had difficulty in correctly discriminating textures rendered with this data-driven method. This system lacked sufficient rendering quality mainly due to the structure of the slider attached to the finger.

Data-driven rendering methods are not limited to a specific parameter. Recorded data could be force, acceleration, velocity, displacement, surface properties, etc. Hover

et al. [116, 117] utilized data-driven method to provide virtual feedback using PHANToM haptic device. It was used to capture material properties when a human operator intuitively explores real deformable objects. The collected data then used to provide haptic feedback.

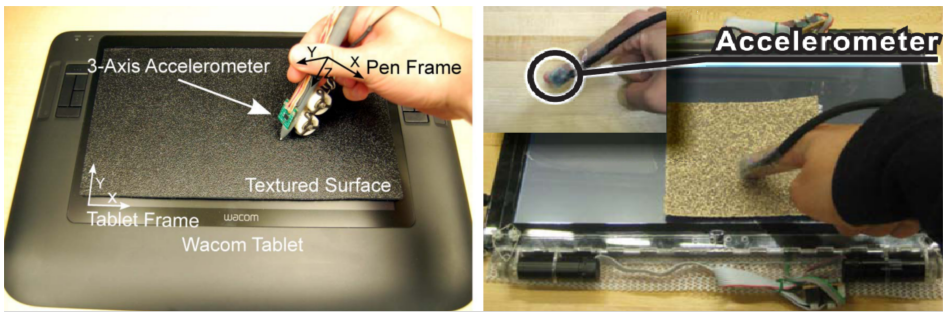

(a) (b)

Figure 2.8. a) An interactive pen is used to collect acceleration signal from surface of the sample materials [112]. b) An accelerometer connected to the finger tip to collect acceleration data [114].

To sum up, data-driven method offers versatile actuation method. It simplifies complicated environment modeling and does not require tedious hand-tuning unlike the conventional method.

3. SINGLE TOUCH ELECTROSTATIC TACTILE SYSTEM

Electrostatic tactile display provides new opportunities to render complex information in touch screen devices. Distinct information patterns (i.e. textures, geometric shapes) can be created in touch screen devices using electrostatic tactile display. This promotes the use of haptic feedback in mobile devices for communicating information between user and the display. In this chapter single touch electrostatic tactile display is introduced. Some preliminary experiments are performed and elicited electrostatic force when finger is in contact with the surface is derived. finally, data-driven rendering method is presented.

3.1. Preliminary Observation on Single Touch Electrostatic Tactile Display

In single touch system induced stimulation on all the fingers is same and uniform. A single touch electrostatic tactile display system was created using a 3M capacitive touch panel (see Figure 3.1). This touch panel is normally used as a single touch capacitive sensor to track finger position, but it is used as a haptic surface in our application. It is composed of a glass substrate, a thin layer of Indium Tin Oxide (ITO) coated on glass, and atop is the Silica (SiO_2) layer which acts as an insulator in contact with the fingertip. AC signal was amplified and applied to the conductive layer.

3.1.1. Effect of Signal Properties on Induced Friction

Electrostatically induced friction force creates a distinct feeling when finger slides over the display. Different signal types such as sinusoidal, square wave, etc. were used to create virtual texture surfaces. Signals were arbitrarily tuned by changing their amplitude, frequency and polarity. Preliminary qualitative analysis on occurred interaction force between finger and surface was revealed that increasing frequency

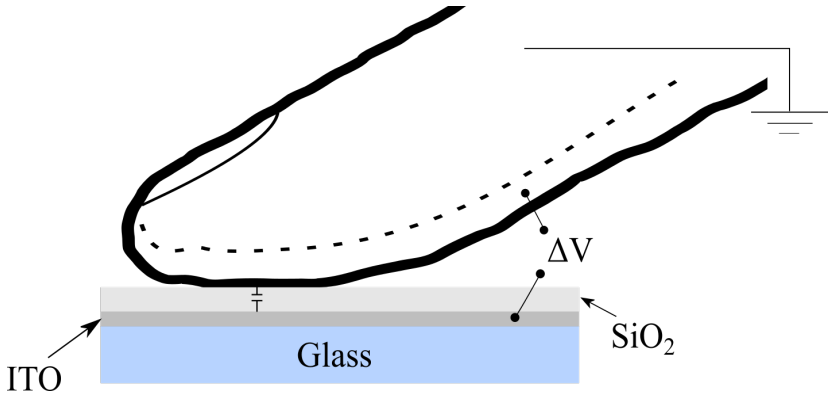

Figure 3.1. A 3M micro touch panel is composed of 3 layers. The outer most insulator layer, Silica (SiO_2) of 1μm thickness, separates the finger from the conductive layer ITO (Thickness = 40 nm).

and amplitude of supply voltage increase friction. Also input signal amplitude can be decreased, if negative polarity signal is used.

3.2. Single Layer Electrostatic Tactile Display Modeling

In order to theoretically calculate electrostatically-induced friction force, a model of electrostatic attraction between a finger and the electrodes is necessary. Given the coefficient of friction (μ) between the finger and the surface, and normal force (F_N) applied by the finger, the total friction force (F_L) is given by:

$$F_L = \mu(F_N + F_E) \tag{3.1}$$

where F_E is electrostatic attraction.

Strong and Troxel [43] were pioneers in introducing a model for an electrostatic attraction force while a finger and an electrically excited conductive plate are in contact. This model is given as:

$$F_E = \frac{\varepsilon_0 A V^2}{2(\frac{T_s}{\varepsilon_s} + \frac{T_r}{\varepsilon_r})^2} \tag{3.2}$$

where ε_0 is the permittivity of vacuum, A is the contact area, and V is voltage between the plate and the finger. ε_s and ε_r are the dielectric constants of the skin (stratum corneum) and of the insulator, respectively. Similarly, T_s and T_r are thicknesses of the skin (stratum corneum) and the insulator, respectively. Agarwal *et al.* [118] emphasized that formulation must contain combination of the insulator layer and stratum corneum layer of the finger tip. Kaczmarek *et al.* [75] has modified this model as:

$$F_E = \frac{\varepsilon_0 A V^2}{2(\frac{T_s}{\varepsilon_s} + \frac{T_r}{\varepsilon_r})(T_s + T_r)} \tag{3.3}$$

Unlike the model proposed by Strong and Troxel (see Equation 3.2) if stratum corneum layer thickness approaches zero in this equation, the result would be the conventional electrostatic force formulation for a single layer capacitor as:

$$F_E = \frac{\varepsilon_0 \varepsilon_r A V^2}{2T_r^2} \tag{3.4}$$

This formula infers that for higher attraction: 1) thickness of the dielectric layer should be as small as possible; 2) the stimulating voltage should be increased; and 3) larger electrode area is needed for greater electrostatic force.

Validation of each proposed formulations might be argued since none of them detailed the finger-surface interface [39]. Let's assume that a bare finger is contact with a single-electrode capacitive tactile display with homogeneous and isotropic dielectric as shown in Figure 3.2. An electric field is formed between the finger and the electrode [119]. Electric field intensity is different for each layer where a dielectric exist. This result in series capacitors which are the capacitances across the insulator (C_r), and the stratum corneum of the finger (C_s) (see Figure 3.2). Total potential difference across the capacitor plates is sum of the potential differences across the dielectric slabs:

$$V = V_r + V_s$$

The total capacitance for two series layers can be written as:

$$C = \frac{C_r C_s}{C_r + C_s}$$

Where $C_r = \frac{\varepsilon_0 \varepsilon_r A}{T_r}, C_s = \frac{\varepsilon_0 \varepsilon_s A}{T_s}$. If charge is constant across each slab, the total charge can be written as:

$$Q = CV = C_r V_r = C_s V_s$$

Using this equation the potential difference across each layer can be calculated as:

$$V_r = V \frac{C}{C_r}$$

$$V_s = V \frac{C}{C_s}$$

We know that electrostatic force across the parallel plate capacitor can be written like:

$$F_E = \frac{C^2 V^2}{2\varepsilon A} \tag{3.5}$$

By substituting the obtained values of voltage and capacitance for each section into Equation 3.5, the induced electrostatic force across capacitor C_r and across capacitor C_s are:

$$F_{E1} = \frac{\varepsilon_0 \varepsilon_r \varepsilon_s^2 A V^2}{2(T_r \varepsilon_s + T_s \varepsilon_r)^2} \tag{3.6}$$

$$F_{E2} = \frac{\varepsilon_0 \varepsilon_r^2 \varepsilon_s A V^2}{2(T_r \varepsilon_s + T_s \varepsilon_r)^2} \tag{3.7}$$

Up to here we ignored the boundary surface between two dielectrics, although

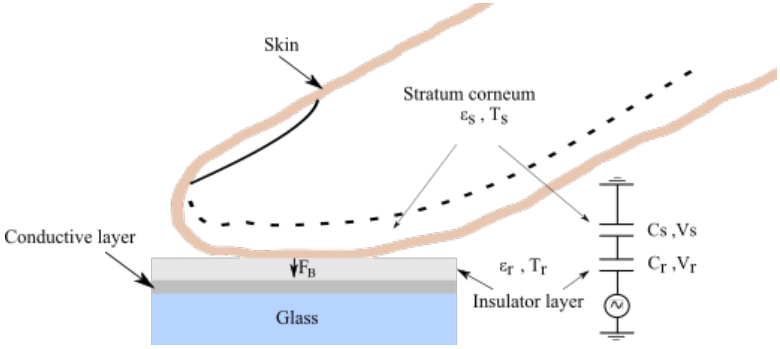

Figure 3.2. Circuit model of an electrostatic tactile display having a single electrode layer.

we assumed that the capacitors are in series. However, there are surface charges on the boundary which separates two dielectrics from each other. To calculate the force on this surface, we can assume that finger and insulator contact region creates an equipotential surface. Voltage is constant on the surface [120]. The boundary force acting on this surface is F_B and is equal to:

$$F_B = F_{E1} - F_{E2} \tag{3.8}$$

where F_{E1} is acting on the boundary of the insulating layer and F_{E2} is the force acting on the boundary of the second insulating layer (stratum corneum).

3.3. Data-driven Texture Rendering with Electrostatic Attraction

In this section, we demonstrate that data-driven texture rendering method can be used to create realistic virtual textures on a touchscreen based on electrostatic attraction. The novel contribution of our study compared to the similar studies [112,115] is that the method is applied to an electrostatic touchscreen [121]. Thus, generated virtual textures can be felt with a bare finger without any intermediary tool or structure between the finger and the screen. The simulated parameter is the roughness. Considering that roughness perception is a result of vibratory stimuli [29, 122], our data-driven method relies on contact accelerations occurring when an object moves on a texture. Although contact force data also provides realistic texture models [123], we

have chosen contact accelerations due to simpler measurements of accelerations from different materials. The recorded acceleration signal is converted to voltage and used for texture rendering on an electrostatic tactile display. Our central hypothesis is that virtual textures rendered with the data-driven method are more realistic in terms of roughness and stickiness than ones generated with periodic signals. The secondary hypothesis in this study is that roughness and stickiness are the primary dimensions in the perception of virtually created textures using electrostatic attraction, because these textures are rendered by modulating surface friction, which creates vibration on the fingerpad as the finger is moved across the surface. These hypotheses are investigated in two main sections. The first part includes proof-of–concept experiments and preliminary analysis in which the data collection setup is introduced, descriptions of the haptic rendering method, and results of psychophysical evaluations. In the second part, as a further investigation of the proposed method, the acceleration dataset provided in the Penn Haptic Texture Toolkit [124] is used as the input signal. This toolkit includes texture models of 100 different materials based on many forces and velocities with uniquely correlated transfer functions. Results of the psychophysical experiments performed on virtual textures created using this second dataset are presented in Part II.

3.3.1. Part I: Data-Driven Texture Rendering

Our data-driven haptic rendering method uses contact accelerations occurring when an object moves on a texture. Unlike similar studies in the literature [112, 115], these acceleration signals, in the form of voltage, are amplified and fed into an electrostatic touchscreen that can be used by a bare finger. In this part, proof-of–concept experiments and analyses are discussed.

3.3.1.1. Sample Materials. Sample materials in our study were cardboard paper (paperboard), hard black plastic, and fiberboard. Note that the rough side (back) of the fiberboard was used in the experiments. Cardboard and plastic were glued on a piece of Plexiglas in order to create similar thickness across all materials. All samples were

prepared to have 20 cm × 15 cm × 0.5 cm dimensions. The materials were selected based on their surface roughness properties and surface texture. Although the sample textures had anisotropic surfaces, they had repetitive asperities in the vertical and horizontal directions. A stylus profilometer (Dektak XTTM, Bruker Corp.) was used to extract surface roughness properties of the materials along the horizontal direction. The profilometer had 4 angstrom repeatability with 1 angstrom height resolution that enabled us to profile repetitive patterns creating roughness. Contact force was set to 3 mg and speed of the stylus was about 250 μm/s. The results obtained with the profilometer were analyzed to calculate a roughness parameter which is the maximum spacing between the profile peaks in the axis of scan. In Figure 3.3, the resulting maximum peak spacing (S_p) values are indicated on the magnified images of the sample materials taken with a stereomicroscope (SMZ1500, Nikon Instruments Europe B.V.). Cardboard has the lowest S_p value (10 μm) and fiberboard has the highest value (1200 μm). All of the samples have greater roughness compared to a glass surface ($S_p \approx 0$ μm). As the perception of roughness is proportional to inter-element spacing of surface gratings [37], we can conclude that roughness increases from cardboard to fiberboard, and plastic has a roughness in between the two. This order was then confirmed by participants of the psychophysical evaluations (see the Psychophysical Evaluation section). In order to measure the surface friction properties of the materials, a tribometer similar to the one reported in [39] has been developed. In the experiments, friction and normal forces between a fingertip and the materials were measured while the finger of a participant was being slid on each material at a constant speed from left to right and in the reverse direction by the tribometer. A six axis force/torque sensor (Nano17, ATI) with 3 mN resolution was chosen to measure the forces at a sampling rate of 1 kHz. The force sensor was attached on the Plexiglas under the materials and fixed firmly to a base. A DC motor was used to move a slider on which the finger was attached using a fastening band. Normal and friction forces were recorded simultaneously in real time and the coefficient of static friction (μ_s) for each sample was calculated in post processing using the peak forces measured in the last 8 reversals. The results showed that μ_s is equal to 0.65±0.04, 1.43±0.18, and 0.70±0.04 for cardboard, plastic, and fiberboard, respectively.

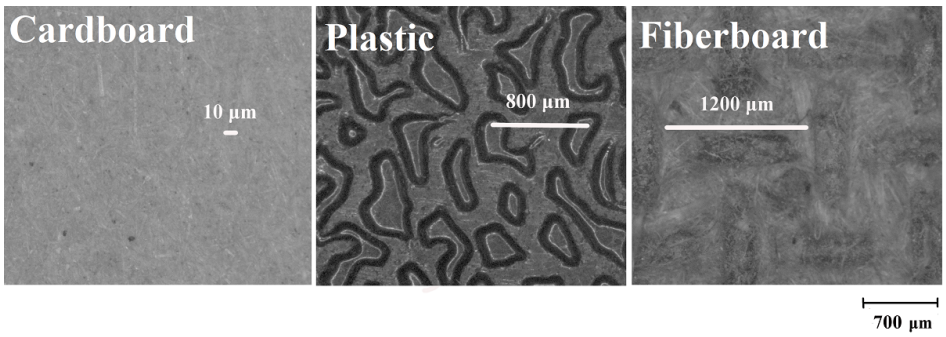

Figure 3.3. Stereomicroscopic images of the sample materials. The maximum peak spacing for each material is indicated. 700 μm is given as a reference.

3.3.1.2. Data Collection. To render realistic surface textures, we have collected contact acceleration data from the three sample materials. The data collection setup shown in Figure 3.4 consists of an accelerometer attached on a Plexiglass bar, and an actuator for motion control of the bar. The actuator was a Dynamixel Ax-12 servomotor having a 0.29° resolution and 254:1 gear reduction ratio. The bar has a semi-triangular shape that is larger at the connection point to the actuator and smaller at the end that carries the accelerometer. The bar was screwed to the motor at four points to firmly deliver motion to the endpoint and was made of 5 mm thick Plexiglas that prevented bending. The natural frequency of the bar was determined as 870 Hz. Motion was controlled by an Arduino Uno board. A tool with a semi-spherical tip was attached to the bar and contacted the sample materials while sliding on a circular path. The spherical tip had a radius of 5 mm and was made of Aluminium. The accelerometer was placed at the tip of the bar to record acceleration signals generated from sliding the tooltip on the samples. The sliding velocity and contact force were constrained during the motion. A force sensor was used to adjust the contact force to 0.35 N during data collection to obtain a consistent force between the tooltip and surface of the samples. The actuator's speed was adjusted such that the tip of the bar slid on the surface with a constant speed (0.74 m/s). Time and distance of travel were constant for all samples. A tri-axial ADXL335 analog accelerometer with a bandwidth of 1600 Hz was used for contact acceleration measurements. Typical sensitivity of the accelerometer in all three directions was 300 mV/G, with zero-G equal to 1.5 V. The Arduino Uno board was

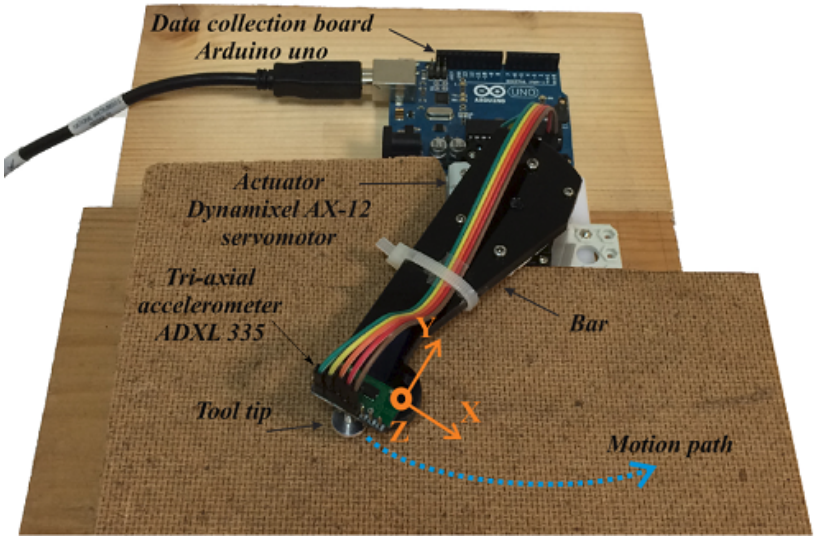

Figure 3.4. Data collection setup. Contact acceleration signals were recorded in two directions. Only the tangential component (X axis) of the accelerations was used for rendering.

used to collect accelerometer output for 200 ms at a sampling rate of 1 kHz.

Two components of acceleration were recorded, but only the X component of acceleration - which is tangential to the motion direction - was used for texture rendering, because it had the largest vibration amplitude [123]. Figure 3.5 shows the X component of the collected stochastic acceleration signals from the samples and their power spectral densities obtained through fast-fourier transforms. The power spectral density shows the frequency content of a signal. As shown in Figure 3.5, the measured signals have distinct forms in the frequency domain. The collected vibration signals unaffected by the resonance of the bar since the largest frequency peaks (i.e., 300 Hz for fiberboard) stays below the first natural frequency of the bar which was determined to be 870 Hz.

3.3.1.3. Electrostatic Force Generation Setup. A capacitive touchscreen (3M Micro Touch) was used as a tactile display to render virtual textures as explained in [15]. In contrast to standard approaches in the literature, each of the collected stochastic

signals from the three samples was amplified and then fed into the tactile display without changing its frequency content. No high frequency sinusoidal or square wave was convolved with lower frequency texture data as in [18,66]. Signals were played repeatedly without changing their frequency characteristics. Two Agilent 33220A function generators were used to generate excitation signals because of their ability to produce a variety of standard signals and play back the recorded data. One of the signal generators was used to save arbitrary signals, and the other was used to produce square waves. Signals amplified by an amplification circuit. The gain of the system was equal to 26 dB.

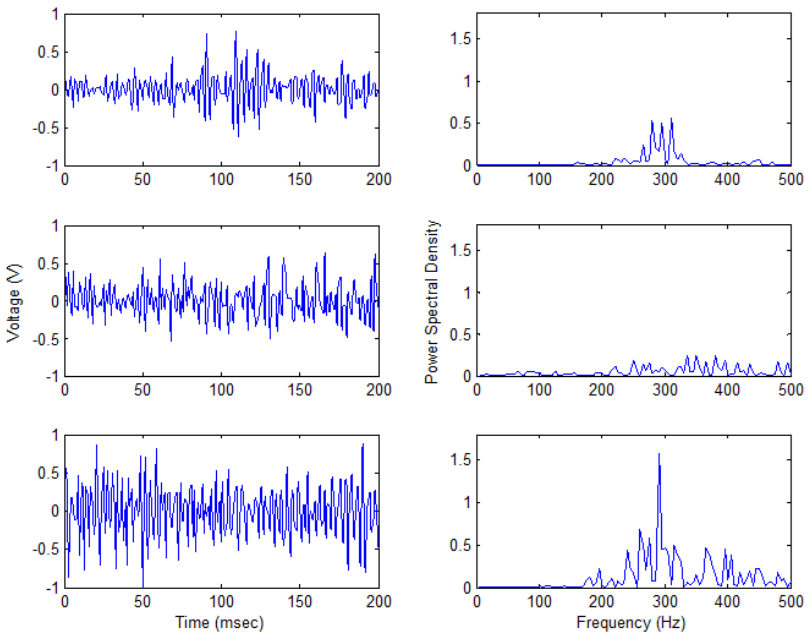

Figure 3.5. Measured accelerations in the form of voltage (Left) are shown for cardboard paper (Top), plastic (Middle), and fiberboard (Bottom) with their frequency contents (Right).

3.3.1.4. Psychophysical Evaluation. We conducted a user study to examine the texture rendering capabilities of our system. Textures (roughness) generated with the data-driven signals were compared with the ones based on square wave signals, and then a perceptual space was created using the multidimensional scaling method. The

Institutional Review Board of Bogazici University approved the experimental procedures. Only three different surface textures (described in the Data Collection section) were used to reduce the number of trials and avoid subject fatigue. Ten participants, including three women (Mean age = 23 years, age range: 20-27 years) and seven men (Mean age = 24 years, age range 20-30 years), gave their written informed consent. All participants were right-handed except one of the female participants. None of the participants had any prior experiences with haptic devices. The data-driven method was compared to the standard method of periodic excitation in terms of realistic roughness rendering. Figure 3.5 shows the signals used for the data-driven method. A square wave signal with a distinct frequency was chosen for roughness rendering through periodic excitation based on the study by Bau *et al.* [15]. In that study, virtually created textures felt smoother as frequency increased with fixed amplitude, and thus frequency was significantly important in surface rendering. High-frequency stimuli (400 Hz) were rated significantly smoother than low-frequency stimuli (80 Hz), and high amplitude stimuli (115 Vpp) were rated less pleasant than lower amplitude stimuli (80 Vpp). Based on these observations, we have chosen 400, 240, and 80 Hz square waves for cardboard paper, hard black plastic, and fiberboard, respectively, in order to render roughness increasing from cardboard to fiberboard. To confirm the effect of frequency on perceived roughness, we studied it in a training session as described in the following section.

3.3.1.5. Experimental Procedure. Before the experimental trials, a training session was performed to familiarize subjects with the experiment procedure. First, each subject was asked to compare all three real materials with each other and comment on their roughness. Second, they were trained on the tactile display. They were asked to slide their index finger on the screen and follow a virtual red dot moving back and forth with a constant speed on a horizontal line. The speed of the red dot was equal to the speed of the sliding bar (described in the Data Collection section) which was 0.74 m/s. This constraint guided subjects to explore the textures at the same speed. They were asked to keep the contact point between their fingertip and the surface constant in order to limit contact force to the range used to touch a tactile display. We set this limit

at $\sim$ 22 - 30 gram (0.2-0.3 N). During the training session, subjects were also asked to comment on perceived roughness on the touchscreen while the frequency of the square wave signal was increased or decreased. During the tests, subjects wore headphones playing white noise to eliminate any surrounding noise and were kept isolated from the electronics of the setup. Subjects were allowed to look at the surfaces they were touching.

3.3.1.6. Scaling of Input Voltage. After the training session, the first part of the experimental trials began. In this phase, the goal was to find the input voltage amplitude preferred by each participant for each sample. Each material was placed beside the touch panel, and subjects were asked to choose whether the virtual or the real sample beside the screen felt rougher, using the staircase method [125]. Amplitudes started from 40 Vpp for the input voltage. If the real surface was selected as rougher, the amplitude of the input voltage was increased by a step size of 8 Vpp. If the virtual surface was selected, the amplitude was decreased by the same amount. By changing the amplitude of the input signals step-by-step, each subject converged to a certain voltage value where he/she felt that the real and virtual surfaces were similar in roughness. This value was considered converged when subjects made four reversals in a row. This experiment was repeated for the data-driven signal and the square wave. Data for each subject was saved and used in the second part of the test.

3.3.1.7. Similarity Rating. In the second part, the goal was to evaluate the quality of the rendered surfaces. Subjects were required to rate the similarity of each virtual texture with each of the real surfaces. At this stage of the experiment, all three samples were placed beside the screen. Subjects compared each virtual texture to the three real samples at the same time and then rated the similarity between them by giving a number between 0 (lowest similarity) and 100 (highest similarity) for each material. Each of the six signals (3 data-driven and 3 square waves) was randomly repeated four times for each subject. After each trial, subjects were required to dry their fingers to avoid sweating. A total of 240 comparisons were completed in this part.

3.3.1.8. Multidimensional Scaling. In the third part, the goal was to study the degree of similarity in perceptual space based on multidimensional scaling (MDS). In MDS space, the distance between two objects reflects their perceptual differences [23, 24, 126]. MDS is an algorithm used to create a perceptual space and get insight into the dimension of stimuli by assigning a point for each stimulus in this space. In this study, we have performed a pair-wise comparison of nine objects (three data-driven textures, three square-wave generated textures, and three real samples) and embedded the results in a multidimensional space. In this step, the setup was the same as before, and each subject was asked to touch a pair of real and/or virtual stimuli. Subjects were required to rate roughness similarity between pairs of nine objects and report a rating between 0 and 100 again. This part of the study was performed by nine subjects (six men & three women) instead of the ten who completed the previous test. Each subject repeated this step three times and performed 135 randomized comparisons in total.

3.3.1.9. Results. Subjects qualitative comments on roughness of each sample material revealed that although cardboard was perceived as uneven due to its microstructure, it was indicated as the smoothest surface among the samples. Plastic had a uniform surface with bumps on its surface. Fiberboard was perceived to be the roughest surface with larger bumps than the other two samples. This roughness order was the same as the one discussed in the Data Collection section. In addition, subjects comments on perceived roughness of the virtual textures rendered with the square wave signal were in agreement with the statement that electrostatically created virtual textures feel smoother as input frequency increases [15]. Results of the psychophysical test are presented in three steps in the following subsections. In our study, "Model" refers to the rendered textures (e.g., Model 1 = Virtual Cardboard) and "Type" refers to the input signal (i.e., data-driven or square wave signal). Overall, the experiments took approximately 75 minutes for each subject, including two 5-minute breaks.

3.3.1.10. Scaling of Input Voltage. The preferred input voltage scaling level for each participant was determined using the staircase method. Figure 3.6 shows the averages

and standard deviations (SD) of the resulting voltages for each Model. Using the average of four last voltage levels as a dependent variable (as discussed in the Experimental Procedure section), the effects of Type (data-driven signal and square wave) and Model (cardboard paper, hard black plastic, and fiberboard) on the converged voltage value for all subjects were analysed. For a total of 60 values (two Types × three Models for ten subjects), a two-way analysis of variance (ANOVA) was performed in SPSS (IBM). This analysis did not find a significant effect of Model on the converged voltage value ($F(2, 59) = 0.688$, $p = 0.507$). On the other hand, Type had a significant effect on the converged voltage ($F(1,59) = 5.74$, $p = 0.02$). The interaction of Type and Model (Type × Model) was not significant ($p = 0.211$).

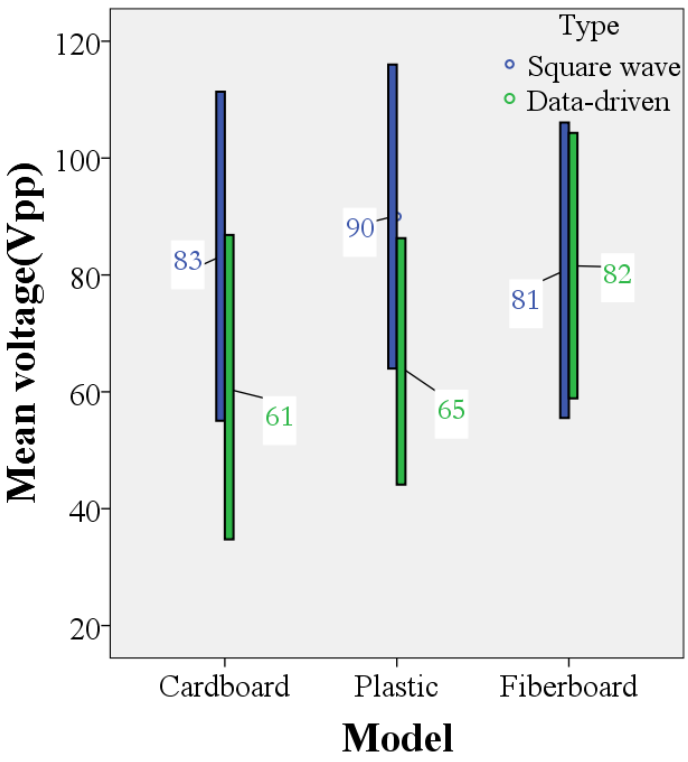

Figure 3.6. Subjects tuned the input voltages to levels at which they found the highest similarity between the real and the virtual textures. Numbers represent mean and standard deviation of the converged voltages over ten subjects.

3.3.1.11. Texture Similarity Rating. In the second part of the experiment, subjects rated similarity of each virtual texture with each real surface, as discussed in the sim-

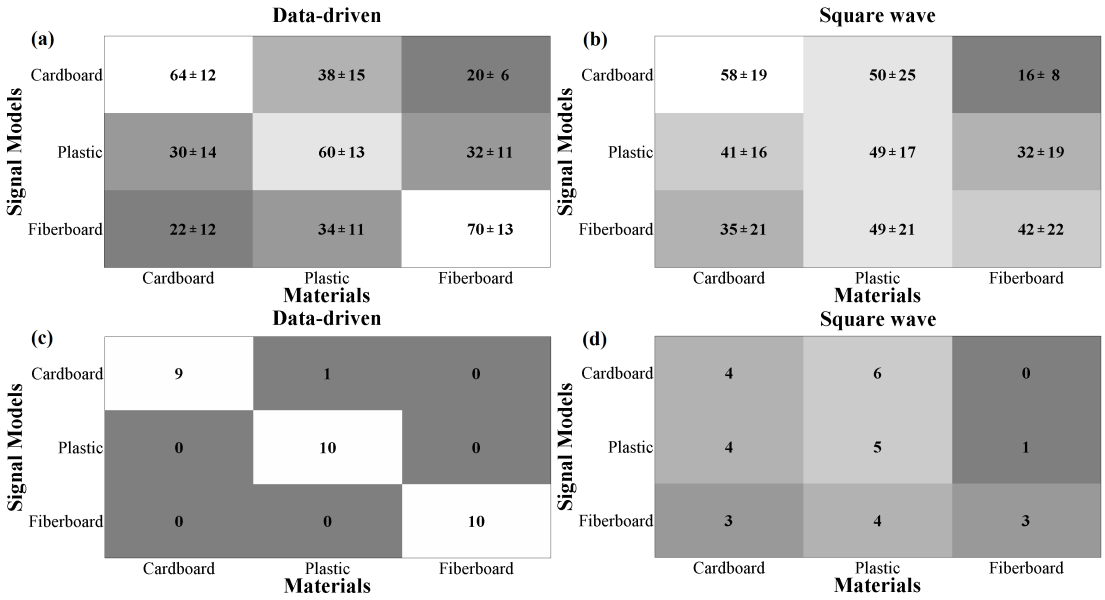

Figure 3.7. Confusion matrices showing (a),(b) similarity ratings and (c),(d) number of the most similar pairs indicated by subjects. In all cases, grey is the lowest rating and white is the highest grade.

ilarity rating section. After taking the average of four repeated similarity ratings of each subject, the mean values and standard deviations of similarity ratings for different models were calculated among all the subjects. Using these results, two confusion matrices were constructed for the data-driven and square wave signals (see Figures. 3.7a & 3.7b). The mean similarity ratings for the data-driven virtual textures and their corresponding materials were higher (> 60) than the ratings for the other materials (< 38) as shown in Figure 3.7a. On the other hand, at least two similarity ratings for each virtual texture rendered with the square wave signal were close to each other (e.g., virtual cardboard was rated as 58 ± 19 and 50 ± 25 for cardboard and plastic, respectively, as shown in Figure 3.7b). Samples with the highest similarity ratings across all subjects were chosen to be the classified materials for the corresponding texture models. The confusion matrices in Figures 3.7c & 3.7d show the number of these classified materials. In other words, the diagonal terms in the matrices represent the number of correct classifications. The sum of each row indicates the number of subjects (ten subjects total). According to the confusion matrix for the data-driven signal (Figure

3.7c), nine subjects classified Model 1 (virtual cardboard) as its corresponding material (cardboard). Only one subject misclassified it as plastic, and no one classified it as fiberboard. All subjects classified Models 2 and 3 as plastic and fiberboard, respectively, without any misclassification. On the other hand, subjects had a considerably higher number of misclassification with the square wave signals (Figure 3.7d). For a clearer comparison, the distribution of similarity ratings for the correct classifications is shown in Figure 3.8 as a box plot. The similarity ratings of each Model for the data-driven signal are higher than the square wave signal. Also, the spans (i.e., the differences between maximum and minimum values) of the similarity ratings are smaller for the data-driven signal than the square wave.

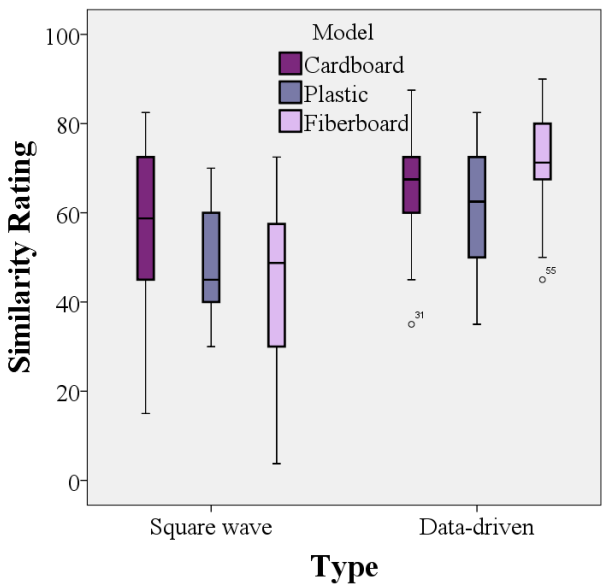

Figure 3.8. Comparison of similarity ratings for the correct classifications. The data-driven method resulted in higher similarity ratings for each model than the square wave rendering.

A three-way ANOVA was performed on 180 recorded values (two Types × three Models × three Materials) for ten subjects. Model, Type and Materials were the independent factors, and similarity rating was the dependent value. The analysis found a significant effect of Type ($F(1,179) = 12.63$, $p = 0.001$) on similarity rating. As a post-hoc analysis, a pairwise t-test was performed on Type for each material. The results showed that Type was not statistically significant in pairwise comparisons for

cardboard and plastic. However, Type was significant for fiberboard ($p = 0.004$).

3.3.1.12. Multidimensional Perceptual Space. MDS analysis was performed using the same statistical analysis software package (SPSS). MDS analysis was carried out based on mutual comparisons of all roughness similarity ratings between pairs of nine objects (reported as a number between 0 and 100). The first step in MDS is to determine number of dimensions in MDS space. A scree plot was used to select a sufficient number of dimensions. According to the scree criteria, the dimensionality at which a sharp elbow is seen in the scree curve is the indication of solution dimensionality [24, 126]. Two dimensions were revealed to be adequate to build an MDS space. As a second step, we formed a perceptual space using the SPSS MDS analysis tool. The resulting MDS perceptual space is shown in Figure 3.9. This figure shows the location of each texture (virtual and real) with respect to each other in the perceptual space. The virtual textures rendered with the data-driven and square wave signals are indicated with "D" and "S" prefixes, respectively. The real samples are shown without a prefix. Distance between two textures reflects their perceptual similarities or differences. Arrows show the Euclidean distances (d) between the virtual textures and their corresponding real textures. According to this graph, d(DCardboard, Cardboard) = 0.45, d(SCardboard, Cardboard) = 0.64, d(DPlastic, Plastic) = 0.39, d(SPlastic, Plastic) = 0.71, d(DFiberboard, Fiberboard) = 0.49, d(SFiberboard, Fiberboard) = 0.82. Please note that the MDS space is unitless. The perceptual space not only gives information about the distance between two stimuli but also provides insight on the perceptual dimensions. In order to identify these dimensions, we needed to put the data points into the most meaningful set of clusters. Three clusters were formed on each dimension based on the location of each data point on the corresponding axis in Figure 3.9. For a better visualization, we used different colors (blue, red, and black) and symbols (star, rectangle, and triangle) to cluster the data points along the first and second dimensions, respectively. The clusters on each dimension were formed by trisecting the range of the data points on the corresponding axis (i.e., each cluster on both dimensions has a width of 0.60 units). The data points in each cluster are located in close proximity on the corresponding axis.

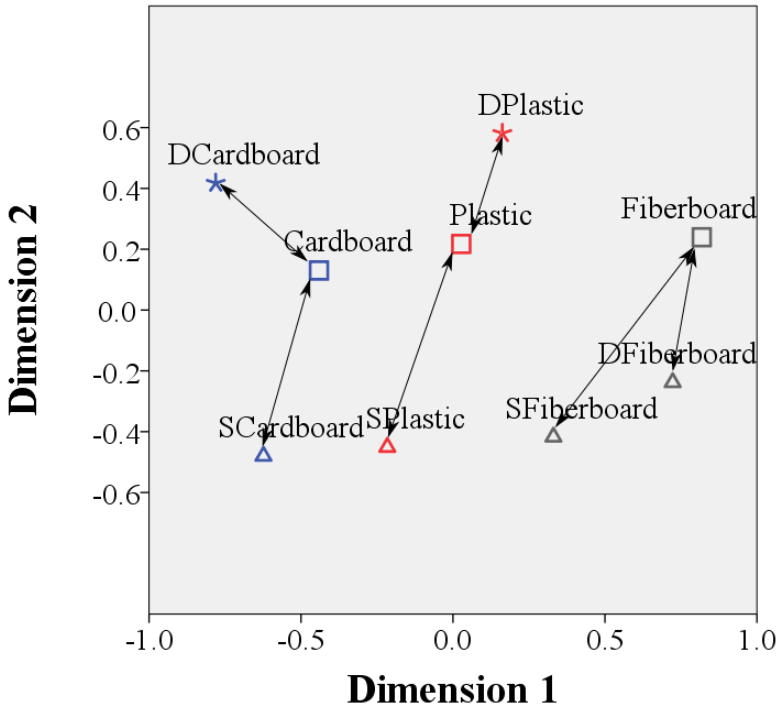

Figure 3.9. Shows MDS perceptual space. Three clusters are formed on each dimension based on colors (blue, red, and black) and symbols (star, rectangle, and triangle) on dimension 1 and dimension 2, respectively.

3.3.1.13. Discussion. According to the results in Figure 3.6, input voltage amplitudes determined by subjects highly depend on the type of signal. For the data-driven input signals, the values of converged voltages are lower than the square wave voltages. It can be concluded from the results of the confusion matrices in Figure 3.7 that fidelity of the data-driven signals is higher than the corresponding square wave signals. Subjects rated the data-driven virtual textures as most similar to their corresponding texture, while the similarity ratings were scattered for the square wave. Also, the numbers of correct classifications were higher for the data-driven signal than the square wave. In addition, as shown in Figure 3.8, the values of similarity ratings for the data-driven models are higher than the ones for the square wave. Please note that we used a 101-point scale (from 0 to 100) instead of a 5 or 7 point Likert scale in order to let the subjects have more freedom in rating the similarities between the textures. However, 101-point scales are known to be subjected to bias responses toward the extremes. Although

this bias reduces their retest reliability, their internal consistency is not significantly affected [127]. In Figure 3.8, the spans of the similarity ratings might indicate the level of a possible bias. Overall ratings span from 10 to 90 and the spans are smaller for the data-driven signal than the square wave. Thus, subjects tended to respond with higher ratings for the data-driven method (e.g., 50 to 90 for fiberboard) than the square wave, which resulted in scattered responses (e.g., 10 to 70 for fiberboard). As shown in Figure 3.8, the virtual fiberboard rendered with the data-driven method had the highest similarity ratings among all of the texture models. Fiberboard has an anisotropic surface with repetitive patterns in the vertical and horizontal directions, as seen in Figure 3.3 (right). However, we collected surface accelerations on a circular path, as shown in Figure 3.4, which may have confused the acceleration response signals. This combination, on the other hand, did not have any negative effect on the realism of the rendered texture, which may be explained by how subjects explored the textures. The typical exploratory procedure for surface texture perception is a repetitive, back-and-forth lateral motion that is not necessarily on a straight line [128]. Since we allowed subjects to freely explore the real surfaces without - firm constraints on exploration path - except the constraints of speed and normal force, they felt the anisotropic surface of fiberboard rather than the repetitive vertical and horizontal patterns. In the MDS analysis, the subjects ratings on similarities between the virtual and real textures resulted in a two-dimensional perceptual space (Figure 3.9). The distance between each virtual model and the corresponding real sample in this space gives information on realism of the rendered texture (the closer to the real sample, the higher the fidelity in texture rendering). All of the data-driven models are located closer to their corresponding real samples than the square wave signals, indicating that the data-driven signals were more successful in representing the natural interactions between the finger and the real materials. This result is compatible with the findings in the texture similarity rating section. According to the ANOVA results, Type was a significant factor when subjects rated texture similarities. The similarity ratings were higher for the data-driven models than the square wave models. The second step in the MDS analysis is to look for a meaningful quality for each dimension. Interpretation of dimensions in MDS relies on identifying what is varying as we move along the

dimensions [113]. In order to do that, the subjective judgments (the data points) in the perceptual space were grouped into three clusters on each dimension based on their location on the corresponding axis. It is inferred from Figure 3.9 that each cluster on dimension 1 contains only one of the three rendered textures (e.g., the red-colored cluster in the middle includes plastic textures). The textures differ from each other in terms of their roughness characteristics. Roughness increases from cardboard to fiberboard, as explained in the data collection section. This order of roughness is also noticeable on dimension 1: cardboard (blue), plastic (red) and fiberboard (black) from left to right. Therefore, we can conclude that the first dimension in the MDS perceptual space is roughness. On the other hand for dimension 2, a meaningful quality that differs between the three clusters seems to be the type of stimuli (i.e., real, data driven, or square wave). This is largely valid, except for the data-driven fiberboard model (Dfiberboard), which is not closer to the other data-driven signals but closer to the square wave signals on dimension 2. All of the sample materials are near to each other on dimension 2. Two of them (cardboard and fiberboard) had friction constants close to each other (see the Data Collection section). Therefore, supposing that the type describes an interaction between the finger tip and the textures, a possible candidate for this interaction is friction/stickiness. To verify this proposition, we need to investigate how stickiness is created for the virtual textures. Stickiness is due to the electrostatic attraction whose intensity is directly proportional to the amplitude of the input voltage. Referring to Figure 4, peak-to-peak mean voltage is about 60 V for the data-driven cardboard and plastic, and 80 V for the fiberboard. On the other hand, all square wave signals have mean amplitudes of about 80 V peak-to-peak. These amplitude values might explain why Dfiberboard is closer to the square wave models on the second dimension. For the reasons outlined above, we can deduce that the second dimension is stickiness. The revealed dimensions, roughness and stickiness, are consistent with the studies on perception of textures in the literature [24, 28, 129]. Our data-driven method was compared with the standard method of periodic excitation, which is typically used for rendering virtual textures. The periodic excitation method relies on trial and error, and Bau *et al.* [15] suggest that virtual textures feel smoother as frequency increases with fixed amplitude. Because of this observation and as roughness

increases from cardboard to fiberboard in our study, we had chosen 400, 240, and 80 Hz square waves for cardboard, plastic, and fiberboard, respectively. The standard practice does not rely on any measurement from real samples. That was the reason why we did not do any signal analysis, and for instance, used dominant frequencies to generate square waves. Otherwise, this would be a kind of data-driven method too. So, the comparison would not be fair. However, it is worth noting that if different fine-tuned frequency and/or amplitude were chosen for the periodic excitation, the results could have been improved. Yet, this point remains to be addressed in a future work. One critical issue to be taken in account while interpreting the results of Part I is the limited number of sample materials. Higher number of materials for measurement and playback were needed to generalize the results. Therefore, a further study was conducted with a larger sample, which is discussed in Part II.

3.3.2. Part II: Application of the HaTT on an Electrostatic Tactile Display

In order to further investigate the validity of the proposed data-driven method, we decided to try other accelerations signals on our electrostatic tactile display. We have used contact accelerations provided in a database available in the literature: the Penn Haptic Texture Toolkit (HaTT) [124]. This database includes 100 different haptic texture models, which have been derived from contact accelerations measured using a pen-like device [113]. The device included sensors to measure high-frequency acceleration while it was dragged across a textured surface [112]. Mathematical models of textures were created for specific normal forces and scanning velocities. In the following subsections, application of the HaTT on the electrostatic tactile display is discussed.

3.3.2.1. Sample Materials from the HaTT. Seven real samples were selected from the HaTT and obtained from the University of Pennsylvania. Figure 3.10 shows the selected materials such as acrylonitrile butadiene styrene (ABS) plastic, medium-density fibreboard (MDF) and leather. These materials cover a large span of surface properties changing in terms of roughness and surface friction. In order to measure their surface properties, we conducted two experiments using the same equipment and meth-

ods described in the Sample Materials section in the Part I of this study. The sample materials were glued on Plexiglas plates before the experiments. First, surface roughness properties were measured. The results (S_p values) obtained from the profilometer are indicated on the stereomicroscopic images of the materials shown in Figure 3.10. Roughness increases from MDF (S_p = 10 μm) to plasticmesh (S_p = 1800 μm), and the others are somewhere in between these two ends. The order of roughness based on these measurements are as follows: MDF, foam, rubber, ABS plastic, leather, vinyl, and plasticmesh. Second, surface friction properties were measured using the tribometer. The results showed that the coefficients of static friction, (μ_s), are 1.06±0.06 for foam, 1.48±0.11 for MDF, 1.50±0.18 for rubber, 1.52±0.08 for plasticmesh, 1.81±0.12 for vinyl, 1.85±0.15 for leather, and 2.02±0.13 for ABS plastic.

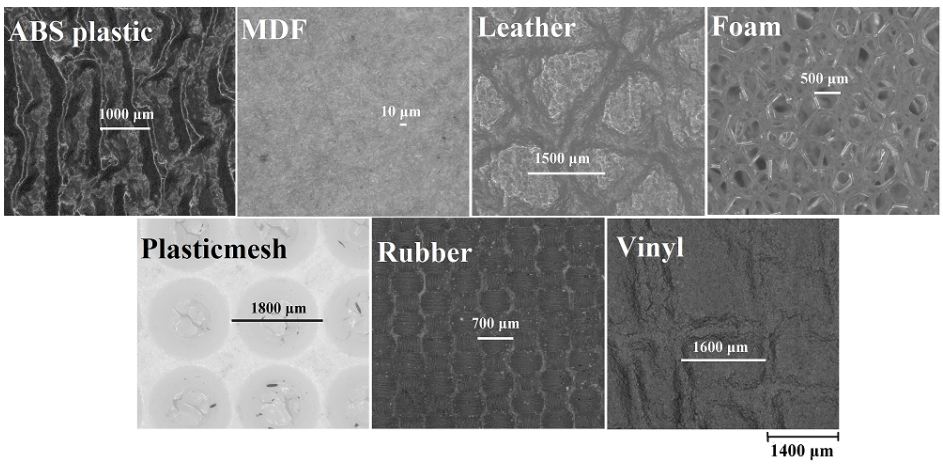

Figure 3.10. Stereomicroscopic images of the materials selected from the HaTT database. The maximum peak spacing for each material is indicated. 1400 μm is given as a reference.

3.3.2.2. Data Processing. Seven texture models, corresponding to the sample materials given in Figure 3.10, were downloaded from the HaTT database. Acceleration signals for each material were obtained from its unique transfer function. Each transfer function is an ARMA (autoregressive–moving average) model whose coefficients are provided in the database for distinct velocities and forces at each vertex of Delaunay triangles [130]. For instance, the Delaunay triangles for the leather model are shown

in Figure 3.11. In stochastic signal analysis, ARMA models provide two polynomials, one for the auto-regression and the second for the moving average, where the output depends on the history of both the past outputs and inputs. An ARMA model corresponds to the following discrete-time transfer function:

$$H(z) = \frac{\sum_{k=0}^{q} c_k Z^{-k}}{1 - \sum_{k=1}^{p} a_k Z^{-k}}$$

Where p is the AR (autoregressive) model order, q is the MA (moving average) model order, and a_k and c_k are the k^{th} AR and MA coefficients, respectively. In the Delaunay triangle shown in Figure 3.11, each vertex represents a single AR or ARMA model at that labeled force and speed. To simplify rendering, the Delaunay triangulation is extended to form a rectangular convex hull by adding linearly spaced models at the maximum modelled force, the maximum modelled speed, the zero force, and the zero speed. To obtain ARMA model coefficients, user's applied normal force and scanning velocity must be measured. Since measuring normal force is not practical on tactile displays, we have assumed a constant normal force of 0.5 N, which corresponds to a light touch according to our preliminary observations with touch screens. Velocities, on the other hand, were determined for ten intervals on the 0.5 N lines through weighted interpolation between upper-bound and lower-bound corners of the triangles.

Transfer functions were built in MATLAB, and the *wgn* function was used to create a white Gaussian excitation signal to input to the ARMA model with a power equal to the interpolated variance value as described in [113]. The resulting model output signals had 1000 data samples in the time domain for constant force and ten velocity intervals. They were saved in a text file for further usage. Similar models from the interaction signals were also proposed by Guruswamy *et al.* [131]. An IR frame having a resolution of 1919 pixels per 512 mm (the spatial resolution is 3.7 pixel/mm) was used to capture the position of the finger. Position and scanning velocity of the finger were recorded and calculated using Labview software. An NI PCIe-6353 data acquisition (DAQ) card was used to play the model output signal on the electrostatic tactile display at 1 kHz. To reach this update rate, only 100 samples of the model

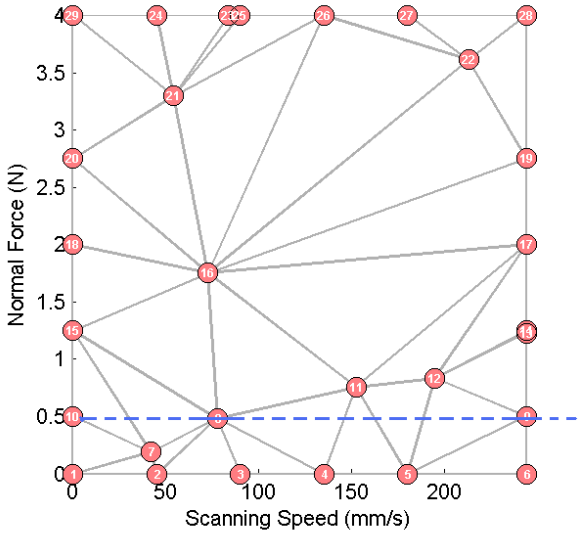

Figure 3.11. Delaunay triangle for the leather model [113]. The dotted line shows the assumed constant normal force. Each vertex represents a single AR or ARMA model at that labelled force and speed.

output were used.

3.3.2.3. User Study. A psychophysical experiment was performed to validate the quality of the rendered virtual textures on the electrostatic tactile display. Ten participants, including five women (Mean age = 24 years, age range: 20-27 years) and five men (Mean age = 25 years, age range: 20-30 years), performed the tests with their written informed consent. All participants were right-handed. None of them had prior experience with haptic devices. The real samples were placed on a table in front of the user. Before the trials, subjects freely explored the samples. Then, they were asked to sort the samples twice: first, regarding surface roughness and second, regarding surface friction. During the tests, subjects wore headphones playing white noise to block any surrounding noise, and they were kept away from the electronics of the setup. They were allowed to look at the surfaces they were touching. In the first part of the user study, only the virtual model of leather was rendered on the tactile display. Leather was used as a reference material to scale input voltage. Subjects were asked to explore both the virtual and the

real leather sample beside the screen and indicate which one felt rougher. The process was started with 42 Vpp, and the staircase method was employed to find the converged scaling value. Unlike the experiment described in the Scaling of Input Voltage section in the Part I, the scaling number was determined for just one sample and used for all the other materials. In the second part of the user study, all seven virtual textures were randomly rendered on the tactile display. Subjects were required to compare all of the stimuli (including virtual textures and real samples) with each other and rate their roughness similarities. They were asked to give a number out of 100, zero being the least similar pair. Total of 91 comparisons were performed randomly, and each subject repeated the task three times. It took about an hour to finish all 273 comparisons.

3.3.2.4. Results. Subjects comments before the experimental trials confirmed that the sample materials differ in terms of both roughness and stickiness. The indicated roughness and friction orders were largely compatible between subjects. Considering the maximum number of times a material selected for a certain place, the orders of the samples were as follows: 1) from smooth to rough: MDF, foam, rubber, leather, vinyl, plasticmesh, ABS plastic; and 2) from slippery to sticky: MDF, foam, leather, rubber, plasticmesh, vinyl, ABS plastic. These subjective results are matched with the results of the profilometer and tribometer measurements (see the Sample Materials from the HaTT section), except for ABS plastic and leather. ABS plastic with a medium roughness was indicated to be the roughest material, while leather was perceived more slippery than what the measurements showed. These differences could be due to the factors such as irregular surface asperities of ABS plastic, and softness of leather, which were not considered in the experiments. Figure 3.12 shows the confusion matrix obtained from the results of the similarity ratings. Columns represent the real material samples and rows represent the virtual models created using the signals of the HaTT. Each element in the matrix shows the number of most similar pairs indicated by the subjects. Therefore, the diagonal elements indicate the number of times that the virtual models were most similar to their corresponding real materials (i.e. correctly classified). For instance; MDF, leather, foam, plastic mesh, and vinyl were mostly classified as their corresponding material. On the other hand, no one classified the virtual model of ABS

plastic as its corresponding material. Instead, it was mostly misclassified as textured rubber. Similarly, eight subjects misclassified textured rubber as MDF.

Figure 3.13 shows similarity ratings between the virtual textures and their corresponding real samples as a box plot. The medians of all these ratings vary between 65 and 75. ABS plastic and rubber have the lowest medians with larger spans. These two virtual models also resulted in poor performance in the confusion matrix (Figure 3.12). There are two outliers in the data related to leather and foam.

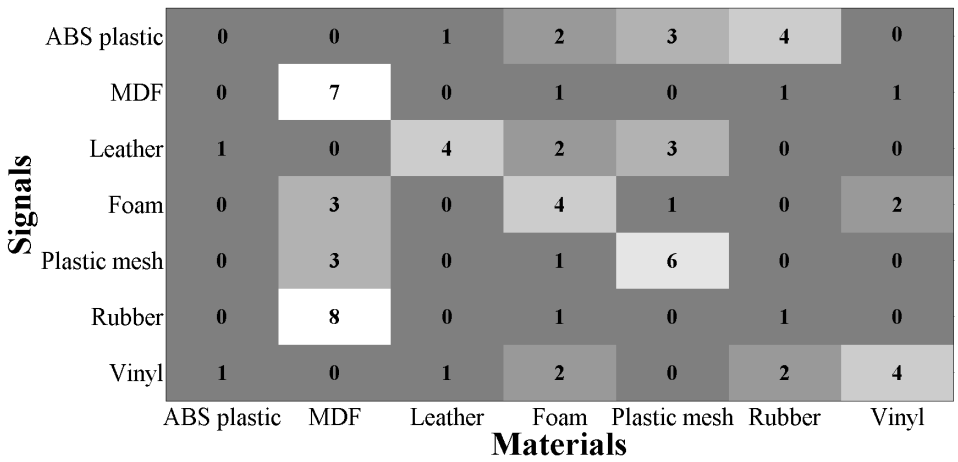

Figure 3.12. Confusion matrix showing the number of most similar pairs. Color encodes numbers from zero (gray) to ten (white).

MDS analysis was performed using SPSS based on mutual comparisons of all similarity ratings between pairs of 14 textures (real and virtual). First, a scree plot was obtained and two dimensions were found to be sufficient to build the corresponding perceptual space. Then, an MDS perceptual space, shown in Figure 3.14, was created using the SPSS MDS analysis tool. The virtual textures rendered with the data-driven signals are indicated with a "D" prefix, while the real samples are shown without a prefix in this Figure The Euclidean distance between each virtual texture and the corresponding real texture is shown with an arrow. According to this graph, d(DABS, ABS) = 1.13, d(DMDF, MDF) = 0.47, d(DLeather, Leather) = 0.37, d(DFoam, Foam) = 0.46, d(DPlasticMesh, PlasticMesh) = 0.60, d(DRubber, Rubber) = 1.03, and d(DVinyl,

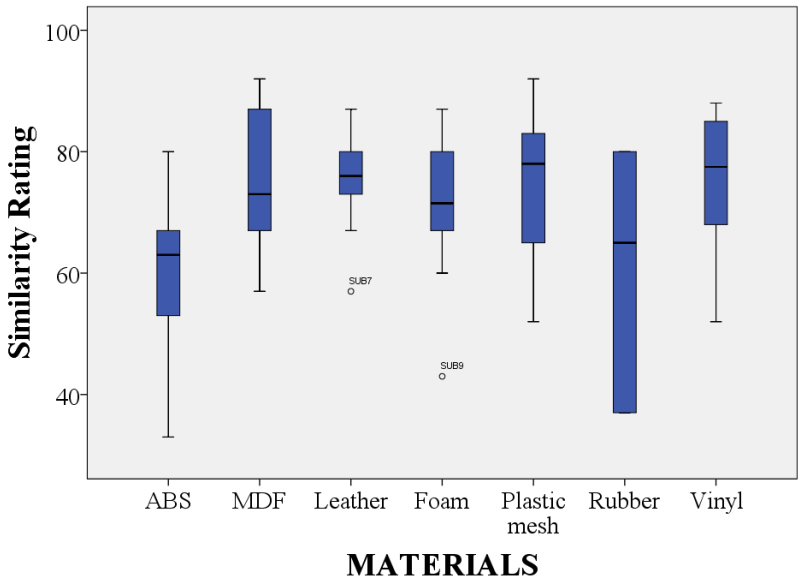

Figure 3.13. Comparison of similarity ratings for the correct classifications between the virtual textures and corresponding real samples. The medians of the ratings is between 65 and 75 for all textures.

Vinyl) = 0.53. We also formed four clusters on each dimension regarding the locations of data points on the perceptual space. Four different colors (blue, green, red, and black) and symbols (star, rectangle, triangle, and circle) were used for the clusters along the first and second dimensions, respectively. The clusters on each dimension have equal widths (0.50 units) and are parallel to each other. The data points in each cluster are close to each other on the corresponding dimension.

3.3.2.5. Discussion. As discussed earlier, proximity between two stimuli in the MDS space (Figure 3.14) reflects their perceptual similarities. In order to define a quantitative benchmark to determine whether a virtual texture feels similar to its real counterpart, we assumed a threshold distance of 0.50 units, which is the width of the clusters. We suppose that if distance between a virtual texture and its corresponding real texture is less than this threshold value, then the virtual texture feels realistic. Applying this benchmark criterion, it is seen that the virtual models of MDF, leather and foam (DMDF, DLeather and DFoam, respectively) were realistically rendered. The

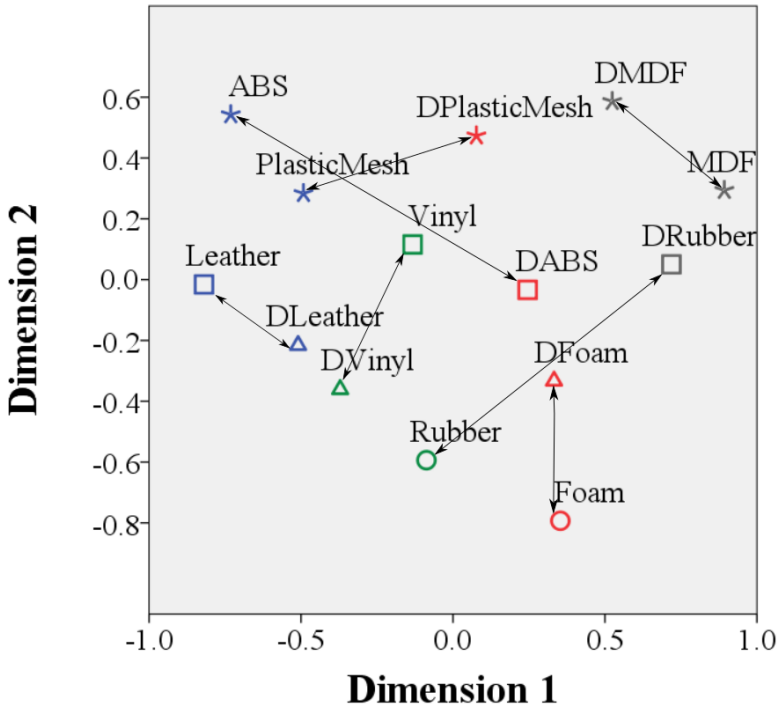

Figure 3.14. MDS perceptual space created through pairwise comparisons of similarity ratings between 14 stimuli. Arrows show distances between the virtual textures and their corresponding real samples.

distances between DPlasticMesh, DVinyl, and their corresponding real materials are slightly above the threshold, indicating that the natural interactions between the finger and these materials were missing some fidelity. On the other hand, ABS plastic and rubber were not rendered effectively at all. In order to interpret the dimensions of the perceptual space, we need to seek qualities changing among the four clusters on each dimension. In addition to the objective measures presented in the Sample Materials section, the subjects' qualitative comments on the sample materials helped us find these qualities. Looking at the distribution of the sample materials on dimension 1 in Figure 3.14, we see that the uneven/rough textures (leather and plastic mesh) are on the left and the smoothest texture (MDF) is on the right. Rubber and foam having medium roughness surfaces are in the middle. Although ABS plastic had medium roughness according to the profilometer measurements, it was rated to be the roughest material by subjects. Therefore, it can be interpreted that the first dimension is roughness. On

the other hand for dimension 2, the texture with the stickiest surface (ABS plastic) is at the top and the driest surface (foam) is at the bottom. Vinyl and leather with sticky surfaces are in the middle. Although the materials having comparable friction constants (plastic mesh, MDF and rubber) are not in the same cluster, these results suggest that a possible candidate for the second dimension is stickiness. This interpretation of the dimension matches with the results obtained in the first part of our study. As discussed in the introduction, roughness stands for the size of surface irregularities and stickiness/friction stands for how much the finger adheres to the surface. In fact, although the task in the user study was to compare similarity in terms of roughness, stickiness was much more dominant for some participants, and they could not focus on roughness, but on friction. There was always some confusion around the concept of similarity ratings of roughness. Most subjects asked, "Should we compare stickiness, bumps, friction, etc.?" Consequently, this altered their judgment. In addition, subjects were able to look at the sample materials they were touching during the tests. Therefore, their judgments might also be influenced by samples appearances. How real textures are distinguished in the absence of visual feedback is a question to be explored in the future. It can be seen from the results of the confusion matrix given in Figure 3.12that the virtually created textures using the acceleration signals of the HaTT were similar to the real samples, although a handheld tool was used to collect vibration signals in the HaTT database [124]. Five out of seven materials have the highest number of similarity ratings on the diagonal elements. Two virtual textures (ABS and textured rubber), which were not similar to their corresponding real materials but to rubber and MDF respectively, need further analysis. These misclassifications are also reflected in Figure 3.14 where virtual ABS (DABS) and virtual textured rubber (DRubber) felt similar to foam and MDF, respectively, in terms of roughness. One reason for these incorrect matches could be that ABS and textured rubber have dense patterns on their surfaces. When these patterns were converted to acceleration signals and then to electrostatic attraction, these high-frequency characteristics might have been damped, and a pattern of smooth surface texture similar to foam and MDF might have been created. In other words, some high-frequency characteristics of the accelerations signals might have been lost during the data acquisition or texture rendering that presented

confusion between some textures. Foam, despite its softness, showed good performance in classification in the confusion matrix and occupied a separate region in the MDS perceptual space. In other words, virtual foam felt very similar to real foam, which is soft. The question arises as to whether soft materials can be rendered with electrostatic attraction. This should be further investigated. While using the HaTT database, we assumed a constant normal force, and only finger velocity was measured. This assumption was valid considering that subjects were asked to keep their normal force constant and moderate. Indeed, a recent study showed that virtual textures using data-driven methods should vary the rendered vibrations with user speed but may not need to vary them with user force in indirect rendering where an intermediary tool is used [132].

3.4. Conclusion

In this chapter, experiments were performed to understand underlying technology of single touch electrostatic tactile display. Qualitative observation by varying input signal amplitude and frequency showed the effect of each parameter in induced friction force between finger and tactile display. Similar observation on polarity showed that input signal amplitude can be lowered if negative polarity is used. Equation 3.4 reveals direct relationship between input signal and induced friction force but does not show anything about the effect of the input signal polarity. The output result of observation performed on the polarity is compatible with the study which notes negative polarity signal causes stronger friction modulation [75]. This result is later used in multi-touch application.

The resultant electrostatic force theoretically calculated when finger is in contact with electrostatic induced tactile display. We emphasized on the occurred force in the finger-surface boundary. We showed that if finger-screen interface is modelled as double layer capacitor, the force is the difference between forces occurs in each part (Equation 3.8). The proposed method based on the parallel plate capacitor theory is compatible with studies [43, 63, 75]. However, studies suggest to model stratum corneum layer as a parallel resistor (R)and a capacitor (C). These studies believe in migration of charges through layers of the fingers at the rate of stratum corneum layer's RC time

constant [39, 88, 133]. In addition, Shultz *et al.* [88] showed that the air gap between the skin and the dielectric material plays a role on the electrovibration as well.

A new method to render realistic textures on electrostatic-based tactile displays has been proposed. Data-driven signals were used to render virtual haptic textures. Acceleration signals occurring due to sliding a rigid probe on a surface were amplified and used as input excitations for an electrostatic tactile display. In the first part, acceleration signals from three different materials were collected with an accelerometer. Acceleration signals were used because it was easier to collect acceleration signals rather than force. However, acceleration signal measured as the voltage and fed in to the display will result in an electrostatic force which is propositional to the square of the voltage and consequently square of the acceleration (look at Equation 3.4). This means that the square root of the data-driven signals must be used instead of directly using data-driven signals to keep voltage-force relationship unchanged. This issue could also be revealed in occurred lateral friction force if spectrum analysis was performed. However, our result showed superior performance of collected signals in comparison to conventional methods even if this problem exists.

The proposed data-driven texture rendering method was compared with standard square wave excitation through psychophysical experiments. The experiments were performed in three stages. In the first stage, input voltage amplitude was scaled for each sample texture to a value preferred by each subject using the staircase method. In the second stage, similarity ratings between real and virtual textures were determined. In the third stage, MDS analysis was performed to create the perceptual space of stimuli. ANOVA tests on similarity ratings showed that Type was a significant factor in texture similarity, where the data-driven method resulted in higher scores. In MDS perceptual space, two dimensions were identified as roughness and stickiness. Shorter distances between the data-driven signals and the real materials in both dimensions suggest higher realism in texture rendering with the data-driven method. According to previous studies, macro textural features are encoded spatially [22,36,38,130,134], and finer features are encoded temporally [135]. Since all of the sample materials in our study had fine textures, we were able to measure and render virtual textures temporally.

Although certain temporal effects, such as instantaneous deformation of the fingertip due to finger compliance, were not considered in the data collection process, our data-driven texture rendering method provided superior realism with respect to the periodic excitation method used in electrostatic tactile displays. This shows that capturing and replaying specific frequency content of surface vibrations - even if it is measured with a rigid tool - are sufficient to create more realistic virtual textures than tuning periodic excitation signals. As a further investigation of the above claim with increased number of samples, we have used contact accelerations provided in a database available in the literature [124]. Acceleration signals adjusted by finger speed were used to render virtual textures on the same electrostatic tactile display. Signals were derived using an ARMA model whose coefficients depended on user force and speed. Although the data collection setup and the tactile display were different than each other, the experimental results of our user study showed that it was possible to generate virtual textures that were highly similar to corresponding real sample materials. Five out of seven textures rendered using the proposed method were correctly classified most of the time. For instance, MDF and plastic mesh showed superior performance even though the measurement setup was a rigid tool. These results showed the feasibility of using the HaTT database to render many textures on a touch panel without any tuning and an intermediate tool. Considering models of 100 materials in the HaTT, the proposed method opens up a cost-effective haptic texture rendering opportunity for the haptics community.

4. MULTI-TOUCH ELECTROSTATIC TACTILE SYSTEM

4.1. Multi-Layer Electrostatic Tactile System

Besides numerous single-touch tactile displays, only a few studies focused on developing tactile displays with localized haptic feedback which is a first step towards multi-touch capability. In nearly all of these studies, an array of conductive electrodes were used to generate haptic feedback. Although previous studies indicated that localized haptic feedback was possible, how multi-point stimulation can be feasibly achieved remains the main problem which must be investigated. Therefore, a new method must be introduced to realize this goal. In this chapter, a new approach to create localized electrostatic forces for multi-touch applications is introduced and fabricated tactile display for this purpose is presented. The induced friction force is measured and evaluated on the points of stimulation. The effect of timing and frequency on measured friction force is investigated. Finally, a user study is performed to measure the performance of the display. Considering voltage level and processing time [93, 136], the developed system is compact and consumes lower energy in comparison to similar studies.

4.2. Tactile Display Prototype

In order to create multi-point stimulation points for multi-touch applications, two orthogonal arrays of electrode lines (on the horizontal X and vertical Y axes) are necessary. Structure of the electrodes is similar to the one found in a projected capacitive (P-Cap) touch sensor, which is a patterned and layered multi-touch sensor [137]. Typically, a P-Cap sensor is composed of interlocking diamond shape electrode lines in rows and columns. A schematic view of proposed system is seen in Figure 4.1. Applying high-voltage AC signals on certain X and Y electrode lines create an electric field between the electrodes and a finger. The field generates an intermittent attractive electrostatic force on the finger when the digit moves over the actuated electrode lines. The amount of increase in friction at these locations can be controlled by changing the amplitude and frequency of the input signals. The result is a perceivable change

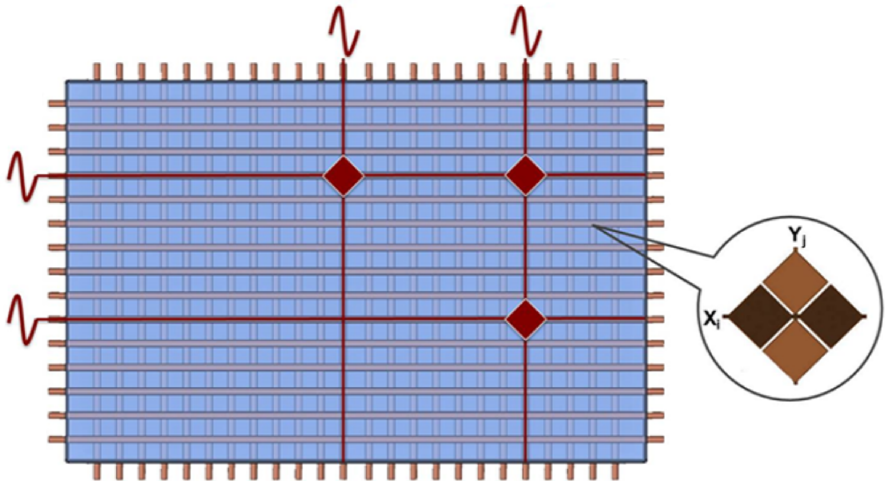

Figure 4.1. Schematic view of the proposed structure for localized haptic feedback. Each line can be controlled separately.

of friction with respect to the neighboring electrodes. This concept was presented in our fist study where electrodes were made from ITO (Indium Tin Oxide) coated PET (Polyethylene terephthalate) to create localized haptic feedback [138].

4.3. Tactile Display

A tactile display prototype for localized multi-touch feedback, which is composed of inter-locking electrode lines, was developed using microfabrication method. There are four main elements in fabrication procedure which must be taken in to consideration before starting clean room process. The selection of the materials was based on availability, cost, process complexity and some design preferences such as flexibility of finger motion, adequate electrode lines and etc.

- **Substrate:** The substrate is a quartz wafer. It was chosen based on its surface specification, thickness and tolerance to heat. It has 100 mm diameter with 0.5 mm thickness.
- **Conductive layers:** There are two choices for material to develope conductive layer in a proposed system.
  (i) Aluminium (Al): has a medium conductivity. It also has an easy deposition

characteristic. It is a cost effective material in the case of repeated process. Also in post-processing steps such as etching, the general etchant such as Aceton could be used. It is not transparent though.

(ii) ITO: is one of the most widely used transparent conducting oxides because of its two chief properties, its electrical conductivity and optical transparency, as well as it can be deposited as a thin film.

- **Insulator layers:** There were two options for developing insulator layers:
  (i) Silicon dioxide (SiO_2): Silica is the typical choice for insulation layer in tactile display industry. It has a good relative permittivity, good insulation property and also uniform surface. Nevertheless it is a little bit hard to do coating process and etching on silica.
  (ii) Parylene-C: is a polymer used as moisture and dielectric barriers. It has relative permittivity as equal as silica. The coating and etching process of Parylene is very simple so makes it a suitable choice for coating purpose.

All the developed prototype during our experiments consists of 17 × 17 lines of Aluminium electrodes arranged in a matrix form. Every line consists of eighteen 2.5 mm × 2.5 mm diamond shape region. The distance between two successive region on a same electrode line is 0.5 mm. (see Figure 4.2)

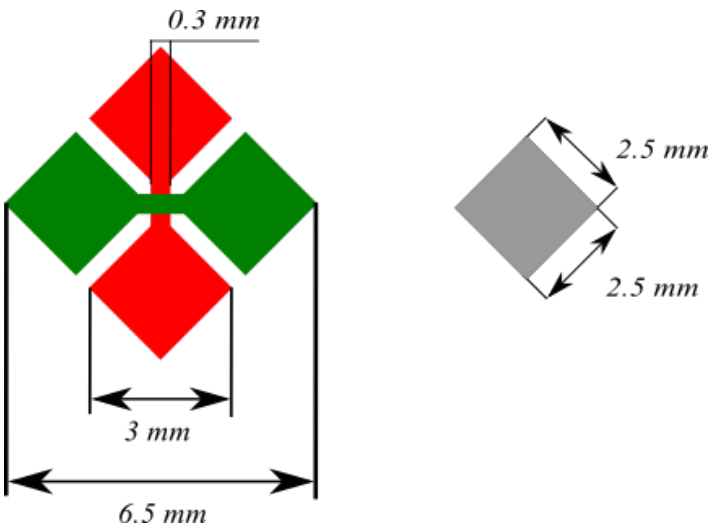

Figure 4.2. Developed electrodes shape and dimensions.

4.3.1. Al Developed Tactile Display Fabrication

4.3.1.1. Double Layers. In the first design the electrode lines were developed in two layers. The X and Y lines of electrodes sits on two different surfaces and insulator layer fills the distance between the X and Y lines of electrodes (see Figure. 4.3). The process is summarized as follows:

(i) Al evaporation: After cleaning the glass wafer, it was placed in the vacuum chamber for Aluminium evaporation. Then, 500 mg Aluminium was put into a tungsten coil and a current of 40 A was applied through this coil to evaporate the Aluminium. This operation was achieved in a pressure of 3×10^{-6} Torr. At the end of the Aluminium evaporation, the samples was coated with Aluminium that had a thickness of around 100 nm.

(ii) Lithography: After Al evaporation, PR (Photoresist) was coated on the surface using spine coating with thickness around 5 μm. Then wafer was soft backed for 2 min under 90°C. UV lithography was done for 2 min with 490 watt power. After this step, wafer was kept in developer (AZ 726 MIF) for 1 min. Since PR patterned, Al surface which was exposed to developer was etched too. Al etching took around 10 min. PR was removed from whole surface using Aceton.

(iii) Parylene-C coating: Parylene coating was done in a vacuum chamber. For 500 nm thickness 1.05 g raw material was used.

(iv) Parts (i) and (ii) were repeated to create second layer of Al.

(v) Part (iii) was repeated.

(vi) Part (ii) was repeated.

(vii) Parylene-C etching: In order to create contact pads RF oxygen plasma was used. The exposure duration was determined experimentally.

(viii) Finally PR was removed from whole surface using Aceton.

4.3.1.2. Single Layer (Bridge typed design). In the second design the electrode lines were developed in a single layer. The X and Y lines of electrodes sit on a same surface. Unlike the previous method the insulator layer in the middle separates diamond shape

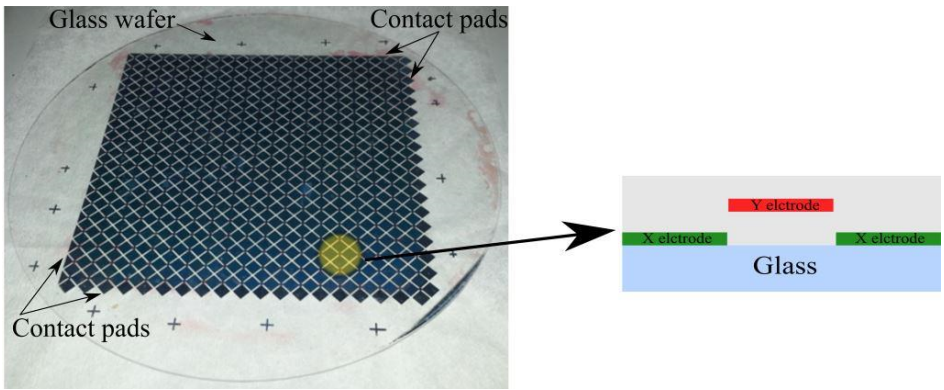

Figure 4.3. Developed tactile display in two layers and its cross section. Electrodes were created using Al.

electrodes connection line like a bridge (see Figure. 4.4). The process is summarized as follows:

(i) Al evaporation: After cleaning the glass wafer, it was placed in the vacuum chamber for Aluminium evaporation. Then, 500 mg Aluminium was put into a tungsten coil and a current of 40 A was applied through this coil to evaporate the Aluminium. This operation was achieved in a pressure of 3×10^{-6} Torr. At the end of the Aluminium evaporation, the samples was coated with Aluminium that had a thickness of around 100 nm.

(ii) Lithography: After Al evaporation, PR (Photoresist) was coated on the surface using spine coating with thickness around 5 μm. Then wafer was soft backed for 2 min under 90°C. UV lithography was done for 2 min with 490 watt power. After this step, wafer was kept in developer (AZ 726 MIF) for 1 min. Since PR patterned, Al surface which was exposed to developer was etched too. Al etching took around 10 min. PR was removed from whole surface using Aceton.

(iii) Parylene-C coating: Parylene coating was done in a vacuum chamber. For 500 nm thickness 1.05 g raw material was used.

(iv) Repeat part (ii).

(v) Parylene-C etching: Parylene-C etched using RF oxygen plasma. The exposure duration is determined experimentally. This stage is done to create bridges.

(vi) Parts (i) to (ii) were repeated to create second conductive layer which passes over the bridges.

(vii) Part (iii) was repeated.

(viii) Part (ii) was repeated.

(ix) Parylene-C etching: In order to create contact pads RF oxygen plasma was used. The exposure duration was determined experimentally.

(x) Finally PR was removed from whole surface using Aceton.

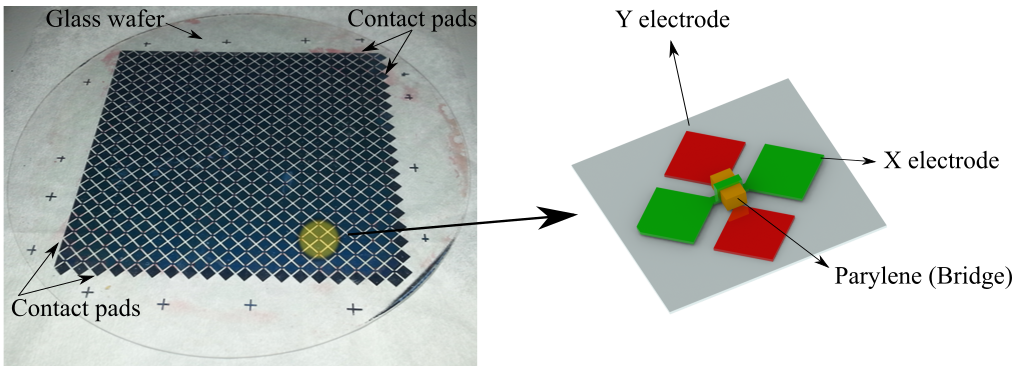

Figure 4.4. Developed tactile display in single layer. Electrodes were created using Al.

4.3.2. ITO Developed Tactile Display Fabrication

4.3.2.1. Double layers. To develop tactile display using ITO, different process was followed. The method is known as Lift-off method. This method was used due to its simplicity and better etching control. In this method, first, PR layer was coated and patterned then the main layer was coated above the PR. While removing PR layer, the main layer was shaped (see Figure. 4.5). The process is summarized as follows:

(i) Lithography: Process is as stated in Sec. 4.3.1.1.

(ii) ITO coating : ITO coating was done using RF sputtering device. The coating pressure was $2-5\times10^{-3}$ Torr. The coating power was 80 watt (2" target). Film growth rate was 4 nm / min. For uniform coating the sample was rotated with longitudinal axis rotation about 10 rpm. Coating was done in room temperature.

Coating was performed in 3 steps. Each step lasted 60 minutes with 90 minutes resting time between them.

(iii) ITO etching: Pr was removed from whole surface using Aceton.

(iv) ITO annealing: Annealing was done for 12 hours under 300° C. The achieved transparency after this step was about 80 percent. Electrode line resistance was around 50Ω.

(v) SiO_2 coating: Silica coating was done in a RF sputtering device. The coating power was 130 watt (2" target). The film growth rate was 1.1 nm / min. Coating was performed in 4 steps. Each step lasted 60 minutes with 90 minutes resting time between them.

(vi) Parts (i) and (v) .

(vii) SiO_2 etching: In order to create contact pads, silica layer must be removed. This was done using hydrofluoric acid (HF). HF was mixed with the water with 20 (water):1 (HF) proportion. This step was not successful since etching process had to be done in a very controlled way.

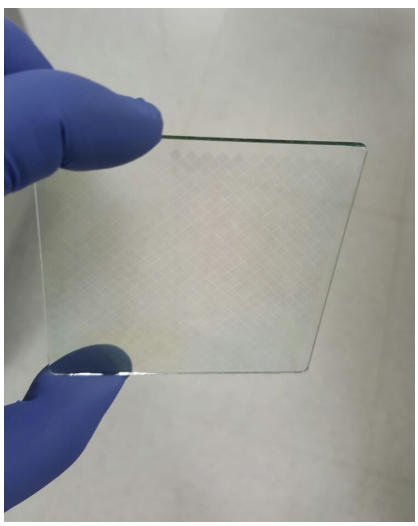

Figure 4.5. Developed tactile display in two layers. Electrodes were created using ITO.

4.3.2.2. Single layer (Bridge typed design). In the second design the electrode lines were developed in a single layer. The X and Y lines of electrodes sit on a same surface. Unlike the previous method the insulator layer in the middle separates diamond shape

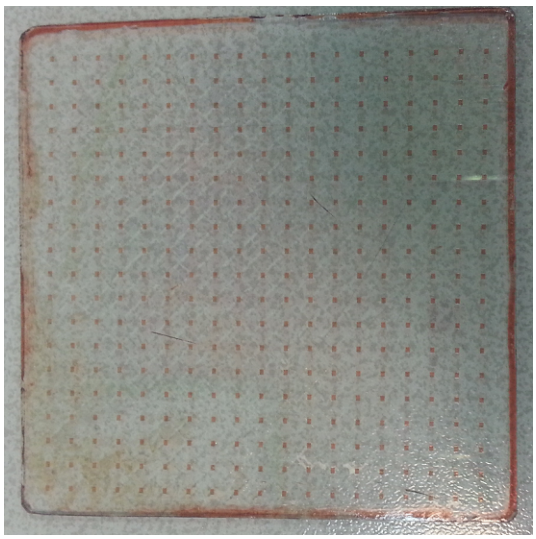

Figure 4.6. The developed tactile display in single layer. The electrodes were created using ITO.

electrodes connection line like a bridge (see Figure. 4.6). The process is summarized as follows:

(i) Lithography: Process is as stated in Sec. 4.3.1.1.

(ii) ITO coating: Process is as stated in Sec. 4.3.2.1.

(iii) ITO etching: PR was removed from whole surface using Aceton (Lift-off method).

(iv) ITO annealing: Process is as stated in Sec. 4.3.2.1.

(v) Parylene-C coating: Parylene coating was done in a vacuum chamber. For 500 nm thickness 1.05 g raw material was used.

(vi) SiO_2 coating: Process is as stated in Sec. 4.3.2.1.

(vii) Parylene-C coating: Part (v) was repeated.

(viii) Lithography: This part was done to mask bridges on the surface. Part (i) was repeated.

(ix) SiO_2 etching: Process is as stated in Sec. 4.3.2.1.

(x) Parylene-C etching: RF oxygen plasma is used to etch Parylene-C from whole surface.

(xi) Parts (i) to (iv) were repeated to create ITO layer lines which passes over the bridges.

(xii) Part (vi) was repeated.

(xiii) Parts (viii) and (ix) were repeated to create contact pads. This step was not successful since etching process must be done in a very controlled way.

4.4. Double Layer Electrostatic Tactile Display Modeling

In order to theoretically calculate electrostatically-induced friction force, a model of electrostatic attraction between a finger and the electrodes is necessary. Similar to procedure which was explained in chapter 3 for single touch system, can be followed to calculate forces due to each layer of electrodes in current proposed structure. In the proposed tactile system we have two layers of conductive layers covered with an insulator. The display explained in section 4.3.1.1 is used for force calculation and texture rendering. While finger moves over electrode lines each of these lines can be treated as single electrode touch system. We neglect mutual and self capacitance. Therefore using superposition method the electrostatic force on each layer can be written as follows:

$$F_{E1} = \frac{\varepsilon_0 \varepsilon_r \varepsilon_s^2 A V^2}{2(T_1\varepsilon_s + T_s\varepsilon_r)^2} + \frac{\varepsilon_0 \varepsilon_r \varepsilon_s^2 A V^2}{2(T_3\varepsilon_s + T_s\varepsilon_r)^2} \tag{4.1}$$

$$F_{E2} = \frac{\varepsilon_0 \varepsilon_r^2 \varepsilon_s A V^2}{2(T_1\varepsilon_s + T_s\varepsilon_r)^2} + \frac{\varepsilon_0 \varepsilon_r^2 \varepsilon_s A V^2}{2(T_3\varepsilon_s + T_s\varepsilon_r)^2} \tag{4.2}$$

where F_{E1} is acting on the first insulating layer due to the first and second layers of the electrodes, and F_{E2} is the force acting on the boundary of the second insulating layer due to the first and second layers of the electrodes. Net force on the boundary can be calculated using Equation 3.8. Contact region area is about 9×10^{-6} m^2 and air permittivity is $\varepsilon_0 = 8.85 \times 10^{-12}$ (see Figure 4.7).

4.5. Input signal characteristics

In order to obtain perceivable tactile stimuli at the desired stimulation point, a sine wave with a frequency of 250 Hz was used as the input signal. The signal was

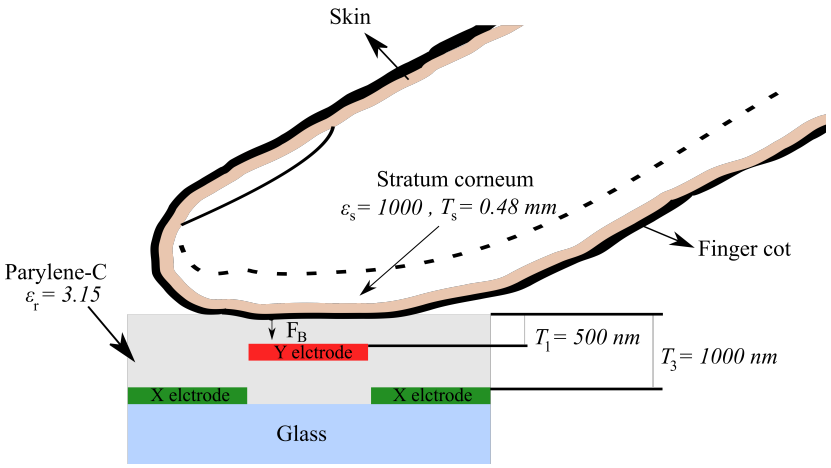

Figure 4.7. Cross section of haptic display having double electrode layers.

adjusted to this frequency because the fingertip is most responsive in the vicinity of this frequency [139]. The signal amplitude was calculated using Equations 4.1, 4.2 and 3.8. Given the Weber fraction for friction discrimination, which is 15% (1.16 dB) [140], an additional force to create a perceivable change in friction at the stimulation point is equal to $\Delta F = 0.15\mu F_N$. Therefore, total friction at the stimulation point is:

$$F_L = \mu(F_N + 0.15F_N) \tag{4.3}$$

Comparing this equation with Equation 3.1, we can see that the additional normal force should be generated by electrostatic attraction between the finger and the display ($F_B = 0.15F_N$). The contact force is assumed to be in a range a user explores a tactile display which is around $\sim$ 0.2 N. Consequently, the electrostatic force at the stimulation point is F_B = 0.03 N. Considering that the electrostatic force is proportional to the square of voltage amplitude (see Equation 3.4), and it is most sensitive to waves with negative polarity [75] and is stronger with a DC offset [77], a negative polarity sine wave with 50 V peak-to-peak amplitude and -25 V DC offset was used.

4.5.0.1. Multiplexing Input Signals. In the proposed row and column construction, each row and column is controlled individually. Therefore, each intersection point creates a unique stimulation point, and thus, tactile feedback is localized. However, when

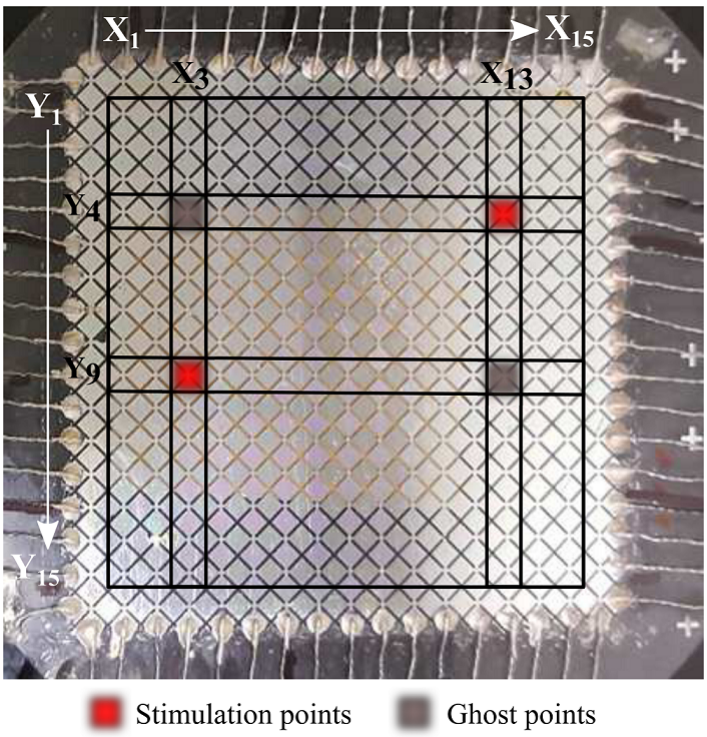

Figure 4.8. Stimulation and ghost points are illustrated in the active workspace (15 × 15 electrode lines corresponding to a surface area of 51 mm × 51 mm) of the prototype.

multiple stimulation points are targeted, additional undesired stimulation points (so called *ghost points*) occur. Figure 4.8 demonstrates this issue for two desired stimulation points. In this example, the target points to stimulate fingers are highlighted with red, which are at the intersections of the activated electrode lines X_3 & Y_9 and X_{13} & Y_4. However, since these electrode lines are excited with the input AC voltage signal, the intersections of X_3 & Y_4 and X_{13} & Y_9 are also stimulated. Therefore, these undesired ghost points are also felt when the display is explored. To solve this problem, we have implemented a multiplexing technique by selectively activating certain electrode lines for a fixed duration, and then deactivating them for the same amount of time. By introducing a phase difference of 90° for activations of the electrode lines, the ghost points are eliminated. In other words, when two perpendicular lines are activated (e.g., X_3 & Y_9), the other two lines are deactivated (X_{13} & Y_4). This process is repeated interchangeably and successively. The activation duration (or, switching time) was determined experimentally as explained in Section 4.6.1. Multiplexing has

been implemented by adding a digital switch to each line, and making them to work in the non-overlapped time slots. Output of each switch was fed in to an amplifier.

4.6. Evaluation

The developed tactile display was evaluated to get both qualitative and quantitative insights about the multi-touch ability.

4.6.1. Quantitative Analysis

Experiments were conducted to measure friction on the display. For this purpose, a tribometer has been developed (see Figure 4.9). The tribometer enables motion in two dimensions (X & Y axes). Most of its parts, such as motor holder, were developed using a 3D printer. Friction forces were measured while sliding an artificial finger horizontally from left to right on the display. A six axis ATI Nano17 force/torque sensor (calibration SI-50-0.5) was chosen to measure the forces. The force sensor was placed under the tactile display, and fixed firmly to the ground. A DC motor (Japon Servo DME34BE50G-108) was used to move a sliding block on a rail above the display with a constant speed. The direction of motion was aligned to the X-axis of the display and the force sensor. Friction forces were measured while sliding the finger horizontally from left to right on the display. The finger was attached to the slider block using a fastening band to obtain constant normal force on the screen. The DC motor was ramped to a predefined velocity to obtain a constant speed of 25 mm/s over the active workspace of the display. Stroke length was 58 mm but width of the active workspace was 51 mm. Normal and friction forces were recorded simultaneously with a sampling frequency of 2 kHz using an NI-PCI 6320 DAQ. Data collection and analysis were performed in Labview and Matlab, respectively. Finger was not electrically grounded throughout the experiments.

Force measurements were performed in the active workspace of the prototype which corresponds to an area of 51 mm $\times$ 51 mm as shown in Figure 4.8. Measurements were taken on each Y electrode from left to right, corresponding to a stroke, and

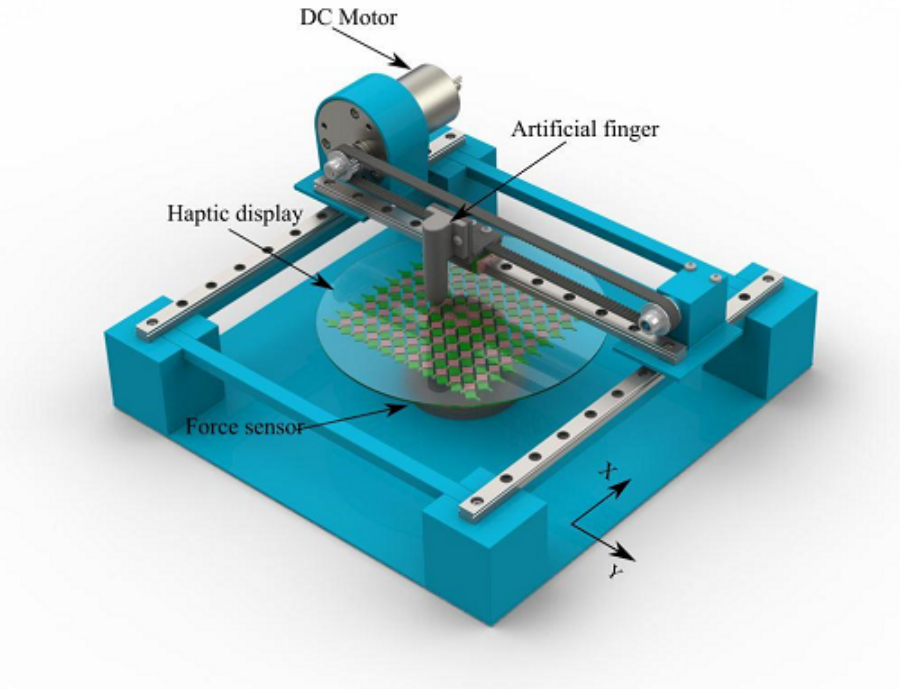

Figure 4.9. Developed tribometer is capable to move in two dimensions (X & Y). The finger is connected to the slider and lateral friction force is collected while moving from left to right.

repeated five times before moving to the next Y electrode. In order to show the change of friction with respect to the location, measurements were analysed in terms of finger position. Each stroke was divided into 15 sections, and average of five repetitions were taken. In the end, a matrix of 15 $\times$ 15 elements were obtained as a friction map on the display. Each element in this matrix represents friction in the corresponding section.

Friction maps were obtained for three conditions: (1) when the display was not activated (i.e., OFF condition), (2) when there was only one stimulation point (i.e., ON condition), and (3) when there were two simulation points (i.e., ON condition, double points). The first condition provides the reference friction values which were used for comparison in the further experiments, and to obtain differential friction maps. The second one shows capability of the display creating a single localized point. Finally, the multiplexing technique for multi-touch ability is examined in the last condition. Before obtaining a friction map, friction on a stimulation point was measured while variables of the multiplexing technique (i.e., input frequency and switching time) were

varied to find an appropriate switching time. All combinations of six frequencies (from 250 Hz to 1500 Hz with increments of 250 Hz) and eleven switching times (from 10 ms to 100 ms with increments of 10 ms, and 200 ms) were tried.

As an example, Figure 4.10 shows measured friction and normal forces while the finger was moved from left to right on a Y electrode line in the OFF and ON conditions. Frequency contents of the measured data, which were determined through Fast Fourier Transform (FFT), are also shown in this figure. The normal force was kept almost constant around ~ 0.2 N during the experiments as seen in Figure 4.10. High frequency vibrations are seen in the friction force in the ON condition. Peaks are observed at the input and harmonic frequencies (250 Hz and 500 Hz, respectively) when signal was ON, as expected for electrostatic displays [77].

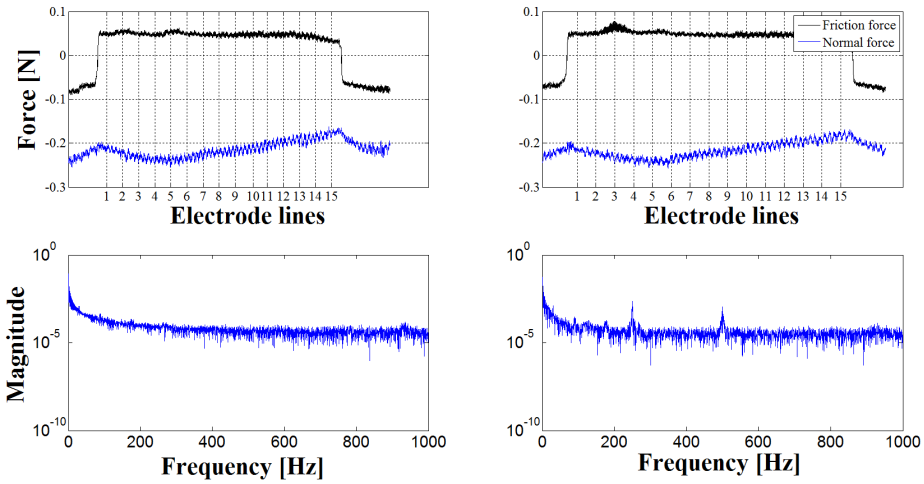

Figure 4.10. Shows collected friction force signal when finger moves from left to right (OFF mode on right; ON mode on the left). FFT analysis of each signal is seen below the each mode.

Friction measurements on a single stimulation point while the multiplexing variables were changed are shown in Figure 4.11. This 3D plot shows friction force for different combinations of the input signal frequency and switching time. The switching time which caused maximum friction was 100 ms at 250 Hz. This value was used in the further experiments.

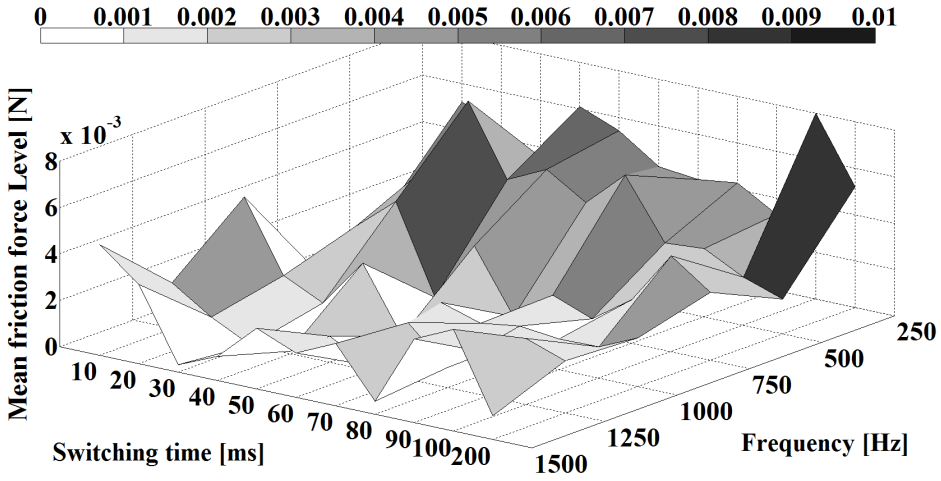

Figure 4.11. Surface representation of the friction force magnitude for different combination of signal frequency and switching time

Differential friction maps were determined by subtracting the obtained friction map in the OFF condition from the ones in the ON conditions. Figure 4.12 shows the differential friction maps for one point (top) and double points (bottom) simulations. As shown in this figure, the friction is higher only at the intended stimulation points.

4.6.2. Qualitative Analysis

We conducted a qualitative user study in order to evaluate how successful the developed display is while rendering a virtual scene with multiple friction patterns. The Institutional Review Board of Bogazici University has approved the experimental procedures. The experimental setup for the user study consists of developed tactile display, a computer screen in which user can see the surface and track his/her finger position using an IR frame (KEYTEC, INC.). All the process were controlled in a PC. Seven volunteers including a woman and six men (Mean age = 24 years, age range 20-30 years), gave their written informed consent. participated in the study after signing the informed consent. All volunteers were graduate student of Bogazici University, and had no prior experience of touching a tactile display. Each participant wore two finger cots on their index fingers, and explored the tactile display with these fingers. The procedure was performed in two stages. First, the participants were asked to

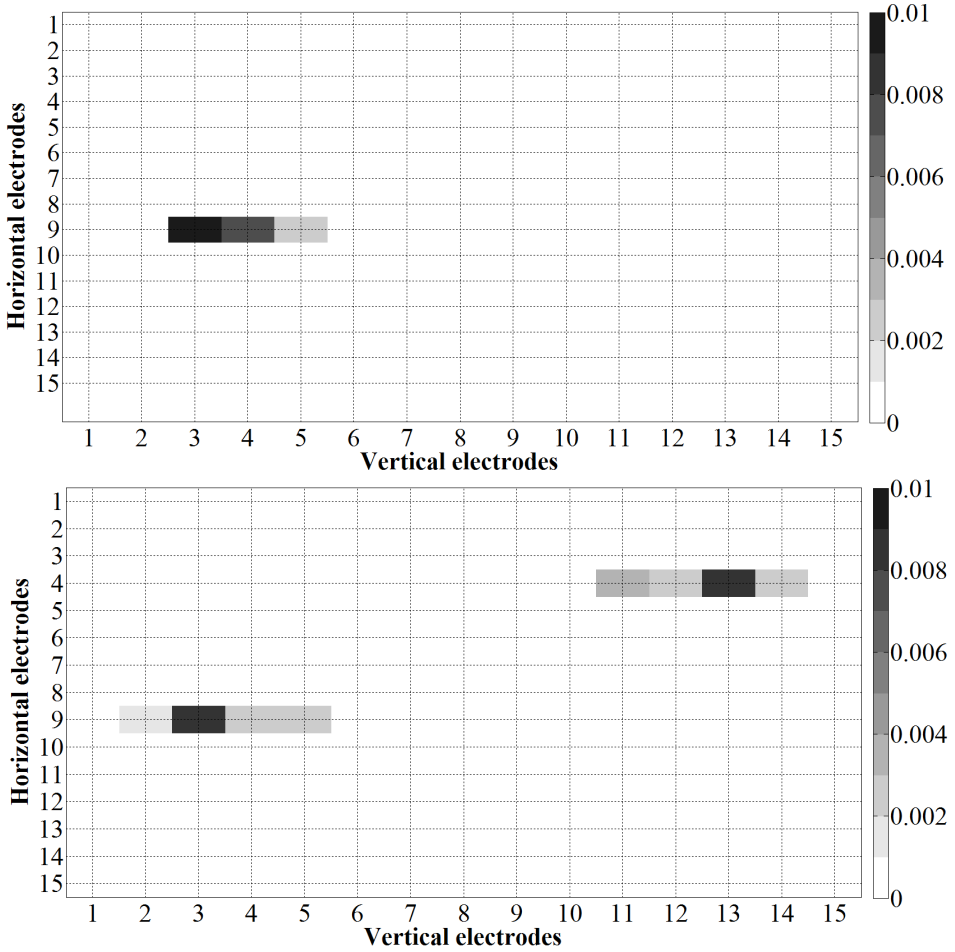

Figure 4.12. Up) Show differential friction map when one stimulation point is selected. Down) show differential friction map when two stimulation points were selected and multiplexing was performed.

freely explore the tactile display surface when signals were OFF in order them to be familiar with the display and screen. In the second stage, a virtual scene containing four different patterns in four regions was shown on the computer screen (Figure 4.13 a), and the corresponding simplified tactile map was rendered on the tactile display (Figure 4.13 b). These four patterns were the horizontal and vertical cracks in the regions one & four, and the bumps in the region two. Two rows and two columns were selected to render these patterns on the four regions. The cracks were rendered with the single horizontal and vertical electrode lines with 100 V peak-to-peak, to make the friction to be perceivable along the lines. The intersections of these lines created the bumps as is shown with circles.

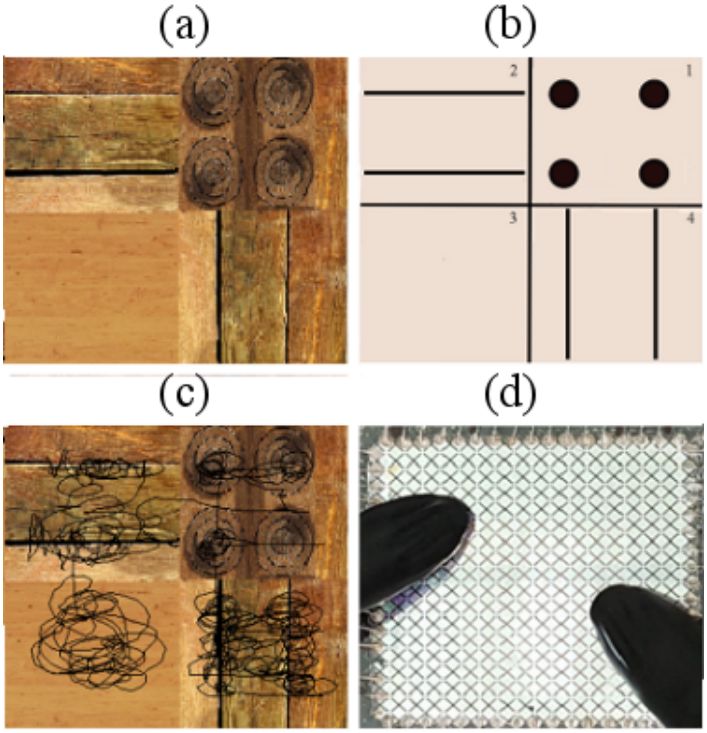

Figure 4.13. a) Specific patterns created virtually. b) The longitudinal pattern such as cracks is rendered using lines. Circles are the point where bumps exist. c,d) Subjects can see and track their fingers path on the screen.

The participants freely explored the virtual patterns with two fingers simultaneously (Figure 4.13 d). They could also see the path followed by the fingers on the screen (Figure 4.13 c). Then, they were asked to fill out a questionnaire including three questions: 1) Do the rendered patterns resemble the corresponding virtual patterns? 2) Do four regions feel different?, 3) Can you distinguish the rendered patterns in four regions from each other?, The participants responded first question using a five-point Likert scale (i.e., 1 = *Not at all* to 5 = *Absolutely*) and they described their experience about the 2nd and 3rd questions verbally. Participants were able to separate the regions from each other. All of them were able to distinguish points inside the regions as well. They recognized direction of the lines inside each region and growth of the friction on the bumps in the 2nd region. Overall they scored rendered pattern recognition 3.85$\pm$0.63 out of 5.

4.7. Discussion

Lateral friction forces were measured on the whole surface of the tactile display using a tribometer. The measured signals were studied in both time and frequency domains. An observation of signals in frequency domain through FFT showed the oscillatory nature of the electrovibration technique. When the system was not excited (input signal was OFF), there was no high frequency oscillation in the measured force signal. On the other hand, an oscillation at about 250 Hz was observed in the friction force when the system was excited with a 50 Vpp, 250 Hz AC input voltage. This conforming to our expectation since adding DC offset to the signal will cause to see the same frequency in the measured friction force. Although the nature of tactile display is looking like an electric antenna, we tried to compensate this issue using thick nonconductive adhesive between force sensor and glass. Also in Figure 4.10 FFT analysis of friction force when the signals are OFF reveals that noise does not affect output signal at least in a range of 250 Hz to 500 Hz where we expect to see oscillation.

The friction coefficient of the display surface was calculated from the data collected when the display was not actuated as described in Section 4.6.1. All the friction values averaged to obtain a mean value for the whole surface (0.048 ± 0.003). Since we can assume a constant normal force ($F_N = 0.2$) the friction coefficient can be calculate as $\mu = 0.25$. Then, the perceivable friction change can also be calculated theoretically as $\Delta F = 0.15 \mu F_N = 0.0075$ N . Experimentally, the largest change of friction that we obtained was 0.009 N at the intersections of the simultaneously-actuated electrode lines. This proves that the induced friction change at the stimulation points were perceivable. In addition, our goal is to keep electrostatic force under perceivable level on the lines heading toward the stimulation points in order to eliminate them. Looking at Figure 4.12 we can conclude that the perceivable friction difference on the actuated lines are smaller than perceivable friction force level (0.0075 N), thus the lines effect were eliminated, too.

We showed that proposed method works for single point (see. Figure 4.12). In case we want to have multiple localized stimulation points ghost points appear thus we

proposed multiplexing technique (see. Figure 4.8) to eliminate these points. Looking at Figure 4.11 we understand that surface friction varies for input frequency and switching time (Multiplexing time interval). It reveals that lower frequencies lead to higher level of friction discrimination force. However in the switching time such a trend hardly can be seen. Then we used 100 ms for switching time at 250 Hz signal frequency. By using these values for stimulation signals we can see in the Figure 4.12 that not only ghost points were eliminated but also we have maximum friction force in desired points and we can use this method for multi-touch application.

In the qualitative analysis, the participants were asked to describe their experience with the rendered patterns in four different regions. All of the participants confirmed that the regions feel different from each other. They were able to distinguish the patterns inside the regions as well. They verified the direction of the lines inside the regions one and four, as well as the location of the bumps in the region two. Answering the first question, they scored a rendered pattern recognition 3.85 ± 0.63 out of five. A user would feel the lines between two bumps in the region two. However, the participants in our study did not figure this out because they mostly focused on bumps, rather than the region around them. As the study has revealed, this problem can be solved through the application of multiplexing.

The developed tactile display is non transparent, but it could be used as a multi-touch trackpad. In order to adapt it to current touch screens, not only transparency must be achieved, but also the resolution of the developed electrode surface must be increased. So that a one-to-one relation between pixel points and stimulation points is obtained. However, smaller electrode size leads to higher voltage requirement and processing time. Therefore, there is a trade-off between resolution and rendering parameters. The proposed method can be adopted to stimulate more than two fingers. However, processing time as well as how fast the system reacts, become important. This will also affect elicit stimulation, as shorter switching time between lines would likely effect temporal stimulation presentation and consequently friction.

4.8. Conclusion

In this chapter, we employed the electrovibration method to create a multi-touch tactile display. For this purpose, we designed and fabricated electrode arrays, with a structure similar to projected capacitive touch sensors used in multi-touch displays. We showed that localized stimulation was achieved by applying high-voltage AC signals on certain X and Y electrode lines. We proposed a multiplexing technique to achieve perceivable friction on multiple desired points. The results were presented through quantitative and qualitative forms. In the quantitative portion, induced friction was measured using the developed 2D tribometer. The result revealed that it is possible to create perceivable change of friction at the multiple intended intersection points while eliminating line and ghost point effects. The qualitative portion required participants to use multiple fingers to explore a virtually created surface with four different patterns. Participants were asked to describe their feelings verbally and to rank whether the rendered patterns resemble the virtual ones. The results revealed that multiple patterns could be rendered at the same time on the display.

5. CONCLUSION

Electrovibration is an emerging method to create tactile feedback in touch screen devices. This thesis utilizes this method to create realistic and multi-touch tactile feedback on touch screens. Therefore two challenges of haptic technology applied to touch screen displays, which are creating multi-touch tactile feedback and realistic texture rendering, are addressed in this thesis.

In Chapter 2, concept of texture was reviewed. Qualities (dimensions or descriptors) which are used to perceive surface texture were defined. Four main qualities (1) rough/smooth, 2) hard/soft, 3) sticky/slippery, and 4) warm/cold) were discussed. Afterwards, roughness was defined based on modes of exploration and surface irregularities. It was stated that roughness perception mechanism for fine and course texture was different, therefore a suitable approach must be taken for surface texture representation. Then, surface haptics was defined and recent developments in this field were presented. Two main technologies to modulate surface friction force were discussed in detail and the pros and cons of each method were discussed thoroughly. Finally, data-driven or measurement based texture rendering method was reviewed.

In Chapter 3, preliminary analyses were performed on a single touch tactile display to understand the basics of electrostatic tactile display technology. Qualitative observation revealed that input signal amplitude, frequency and polarity were the three main parameters in texture rendering based on altering surface friction force. Negative polarity signal was seen to lower the input voltage amplitude. Then, using parallel plate capacitor model, an electrostatic force on a single touch system was calculated. Note that it would be better to consider skin resistance in the modelling and perform an impedance analysis. In this case impedance of an air gap between finger and the surface must be considered too. Data-driven method as a new method to generate and render surface texture was introduced. The method based on contact acceleration signals was showed to be an alternative for current trial and error surface texture rendering methods. Novelty of the approach is that no intermediary tool is used, and

the collected acceleration signals are directly used to create haptic feedback on a bare finger. The results presented in two parts proving the feasibility of this method.

In Chapter 4, one of the most important shortcomings in electrostatic tactile display, which was creating localized multi-touch haptic feedback, was addressed. In a single touch tactile system, only one finger can be used. To stimulate more than one finger first, a new display was fabricated which was composed of an array of interlocking electrodes. The findings in Chapter 3 were used to determine the proper stimulation signals. It was showed that if finger passes over the point where actuated horizontal and vertical electrodes cross, a distinct localized feeling can be created. The approach was extended to multi-touch applications by introducing a multiplexing technique. With this approach, not only ghost points were eliminated, but also two distinct stimulation points were created. The method was evaluated quantitatively and quantitatively. The developed 2D tribometer was used to measure friction force on the display. In quantitative analysis, a user study was performed to evaluate how the developed tactile display can render a virtual surface composed of lines and dots? Both quantitative and qualitative analyses revealed that the proposed structure and the actuation method can be implemented in touch screen devices after an improved fabrication process. Although the developed tactile display is non transparent, it opens a way for research groups which want to investigate different aspect of display such as electrode size, insulator thickness, electrode pitch size, different electrode shape and configurations.

5.1. Contribution to the Literature

The results of the thesis was presented in the two international conferences (Eurohaptics 2014, World-haptics 2015) [141, 142] and submitted to the Haptic-Symposium 2018 international conference. Also, it is presented in a local project showcase (TET ProjeBahari 5). A workshop was organized to present what we have achieved on data-driven texture rendering at the World-haptics 2017. In addition we successfully published a paper at the International Journal of Human-Computer Interaction [143].

5.2. Future Work

This study experimentally showed that the developed display allows us to create multi-point localized haptic feedback, and the data-driven method have a capability to be used in electrostatic tactile displays as a mean for realistic haptic rendering.

Qualitative experiments on the effect of polarity on surface texture perception were performed. Although studies [75, 77] addressed this, further experiments is necessary to understand why finger skin shows lower sensitivity threshold to negative polarity signal?

In Chapter 3.3 part I, the interaction acceleration signals were collected using a rigid tool. Collected signals then replayed on tactile display. As a more logical way, acceleration signals can be collected while bare finger explores surface of the materials. An accelerometer must be connected to the finger for this purpose. However, other issues such as positioning accelerometer, finger deformation would appear. Another issue which must be considered is the conversion of the acceleration signals to voltage as discussed in Sec. 3.4. The type of the collected signals is also matter of interest. Which of the signals such as surface shape signal, interaction force, interaction velocity and, acceleration could lead to a better performance is still unknown and can be investigated in future research.

Multi-touch haptic display was developed and its performance to create electrostatic force was presented. Using materials like SiO_2 for insulator layer needs a very precise procedure. These issues must be considered prior to fabrication. A finite element simulation could be helpful to understand the exact behaviour of single and double layers tactile display . Doing this, optimum electrode area, pitch size etc. can be extracted. Modelling based on parallel plate capacitor would probably not be sufficient. Exact electrical modelling considering source impedance, conductivity of insulator layers and structure of the finger would be beneficial.

5.3. Outlook

The proposed methodology for data-driven rendering is a major step toward wide spread use of this method in haptic rendering in touch screen devices and in a generic context can be applied to many types of haptic interfaces. It not only simplifies rendering issue in touch display devices but also leads to a richer and compelling way of rendering. Although, feasibility of using HaTT data base for rendering was approved in this study but in the future a library can be prepared for haptic community by adding other information to database such as compressibility.

The proposed tactile display to achieve multi-touch haptic feedback is a method compatible with current industrial-scale manufacturing of capacitive touch screen devices. Although, it is fully adaptable to current state of touch display devices, to validate the developed tactile display proper use in the current touch displays is required. Current measurements alone will likely not be sufficient so in-depth analysis are still required to understand the exact behaviour of the display.

REFERENCES

1. MacLean, K. E., "Putting haptics into the ambience", *IEEE Transactions on Haptics*, Vol. 2, No. 3, pp. 123–135, 2009.

2. Hayward, V. and O. R. Astley, "Performance measures for haptic interfaces", *Robotic research-International Symposium*, Vol. 7, pp. 195–206, MIT Press, 1996.

3. McMahan, W. and J. Gewirtz, "Tool contact acceleration feedback for telerobotic surgery", *IEEE Transactions on Haptics*, Vol. 4, No. 3, pp. 210–220, 2011.

4. Chouvardas, V., A. Miliou and M. Hatalis, "Tactile displays: Overview and recent advances", *Displays*, Vol. 29, No. 3, pp. 185–194, July 2008.

5. Siegel, E., "Haptics technology: picking up good vibrations", `https://www.eetimes.com`, 2014, accessed at December 2017.

6. "Multi-touch", `https://www.wikipedia.org/`, 2014, accessed at December 2017.

7. Taylor, P., A. Moser and A. Creed, "A sixty-four element tactile display using shape memory alloy wires", *Displays*, Vol. 18, No. 3, pp. 163–168, May 1998.

8. Levesque, V., L. Oram, K. MacLean, A. Cockburn, N. D. Marchuk, D. Johnson, J. E. Colgate and M. A. Peshkin, "Enhancing Physicality in Touch Interaction with Programmable Friction", *Proceedings of the SIGCHI Conference on Human Factors in Computing Systems*, CHI '11, pp. 2481–2490, ACM, New York, NY, USA, 2011.

9. Wagner, C. R., S. J. Lederman and R. D. Howe, "A tactile shape display using RC servomotors", *Proceedings 10th Symposium on Haptic Interfaces for Virtual Environment and Teleoperator Systems. HAPTICS 2002*, pp. 354–355, 2002.

10. Liu, Y., R. Davidson, P. Taylor, J. Ngu and J. Zarraga, "Single cell magnetorheological fluid based tactile display", *Displays*, Vol. 26, No. 1, pp. 29–35, January 2005.

11. Sarakoglou, I., N. Tsagarakis and D. Caldwell, "A Portable Fingertip Tactile Feedback Array-Transmission System Reliability and Modelling", *First Joint Eurohaptics Conference and Symposium on Haptic Interfaces for Virtual Environment and Teleoperator Systems*, pp. 547–548, IEEE, 2005.

12. Laitinen, P. and J. Mawnpaa, "Enabling mobile haptic design: piezoelectric actuator technology properties in hand held devices", *2006 IEEE International Workshop on Haptic Audio Visual Environments and their Applications (HAVE 2006)*, Vol. 9, pp. 40–43, 2006.

13. Fukuda, T., H. Morita, F. Arai, H. Ishihara and H. Matsuura, "Micro resonator using electromagnetic actuator for tactile display", *1997 International Symposium on Micromechanics and Human Science*, pp. 143–148, 1997.

14. Kajimoto, H., N. Kawakami, T. Maeda and S. Tachi, "Tactile feeling display using functional electrical stimulation", *Proc. 1999 ICAT*, p. 133, 1999.

15. Bau, O., I. Poupyrev, A. Israr and C. Harrison, "TeslaTouch", *Proceedings of the 23nd annual ACM symposium on User interface software and technology - UIST '10*, p. 283, ACM Press, New York, New York, USA, 2010.

16. Wijekoon, D., M. E. Cecchinato, E. Hoggan and J. Linjama, "Electrostatic Modulated Friction as Tactile Feedback: Intensity Perception", Poika Isokoski and Jukka Springare (Editors), *Haptics: Perception, Devices, Mobility, and Communication*, pp. 613–624, Springer Berlin Heidelberg, 2012.

17. Bau, O. and I. Poupyrev, "REVEL: Tactile Feedback Technology for Augmented Reality", *ACM Transactions on Graphics*, Vol. 31, No. 4, pp. 1–11, July 2012.

18. Kim, S.-C., A. Israr and I. Poupyrev, "Tactile Rendering of 3D features on Touch Surfaces", *Proceedings of the 26th annual ACM symposium on User interface software and technology - UIST '13*, pp. 531–538, ACM Press, New York, New York, USA, 2013.

19. Hover, R., M. D. Luca and M. Harders, "User-based evaluation of data-driven haptic rendering", *ACM Transactions on Applied Perception*, Vol. 8, No. 1, pp. 1–23, October 2010.

20. Lang, J. and S. Andrews, "Measurement-based Modeling of Contact Forces and Textures for Haptic Rendering.", *IEEE transactions on visualization and computer graphics*, Vol. 17, No. 3, pp. 380–91, March 2011.

21. Bott, R., *haptic rendering foundations algorithms and applications*, A K Peters, Ltd., 2008.

22. Johnson, K. O., S. S. Hsiao and T. Yoshika, "Neural Coding and the Basic Law of Psychophysics", *Neuroscientist*, Vol. 8, No. 2, pp. 111–121, 2002.

23. Jones, L. A. and H. Z. Tan, "Application of Psychophysical Techniques to Haptic Research", *IEEE Transactions on Haptics*, Vol. 6, No. 3, pp. 268–284, July 2013.

24. Hollins, M., R. Faldowski, S. Rao and F. Young, "Perceptual dimensions of tactile surface texture: A multidimensional scaling analysis", *Perception & Psychophysics*, Vol. 54, No. 6, pp. 697–705, November 1993.

25. Yoshida, M., "Dimensions of tactual impressions (1)", *Japanese Psychological Research*, Vol. 10, No. 3, pp. 123–137, 1968.

26. Shirado, H. and T. Maeno, "Modeling of human texture perception for tactile displays and sensors", *Proceedings - 1st Joint Eurohaptics Conference and Symposium on Haptic Interfaces for Virtual Environment and Teleoperator Systems; World Haptics Conference, WHC 2005*, pp. 629–630, 2005.

27. Guest, S., J. M. Dessirier, A. Mehrabyan, F. McGlone, G. Essick, G. Gescheider, A. Fontana, R. Xiong, R. Ackerley and K. Blot, "The development and validation of sensory and emotional scales of touch perception", *Attention, Perception, & Psychophysics*, Vol. 73, No. 2, pp. 531–550, 2011.

28. Okamoto, S., H. Nagano and Y. Yamada, "Psychophysical Dimensions of Tactile Perception of Textures", *IEEE Transactions on Haptics*, Vol. 6, No. 1, pp. 81–93, January 2013.

29. Yoshimoto, S., Y. Kuroda, M. Imura and O. Oshiro, "Material Roughness Modulation via Electrotactile Augmentation", *IEEE Transactions on Haptics*, Vol. 8, No. 2, pp. 199–208, April 2015.

30. Yoshioka, T., J. C. Craig, G. C. Beck and S. S. Hsiao, "Perceptual Constancy of Texture Roughness in the Tactile System", *Journal of Neuroscience*, Vol. 31, No. 48, pp. 17603–17611, November 2011.

31. Lederman, S. J. and R. L. Klatzky, "Haptic perception: A tutorial", *Attention, perception & psychophysics*, Vol. 71, pp. 1439–1459, 2009.

32. Jones, L. A. and S. J. Lederman, *Human hand function.*, Oxford University Press, 2006.

33. Klatzky, R. L. and S. J. Lederman, "Tactile Roughness Perception With a Rigid Link Interposed Between Skin and Surface", *Perception & Psychophysics*, Vol. 61, No. 4, pp. 591–607, January 1999.

34. Wiertlewski, M., *Reproduction of Tactual Textures*, Springer Series on Touch and Haptic Systems, Springer London, London, 2013.

35. Lederman, S. J., R. L. Klatzky, C. L. Hamilton and G. I. Ramsay, "Perceiving Roughness Via a Rigid Probe: Psychophysical Effects of Exploration Speed and Mode of Touch", *Haptics-e*, pp. 1–20, 1999.

36. Yoshioka, T., S. J. Bensmaia, J. C. Craig and S. S. Hsiao, "Texture perception Through Direct and Indirect Touch: An Analysis of Perceptual Space for Tactile Textures in Two Modes of Exploration", *Somatosensory & Motor Research*, Vol. 24, No. 1-2, pp. 53–70, January 2007.

37. Lawrence, M. A., R. Kitada, R. L. Klatzky and S. J. Lederman, "Haptic roughness perception of linear gratings via bare finger or rigid probe", *Perception*, Vol. 36, No. 4, pp. 547–557, 2007.

38. Klatzky, R. L. and S. J. Lederman, "Multisensory Object Perception in the Primate Brain", pp. 211–230, 2010.

39. Meyer, D. J., M. A. Peshkin and J. E. Colgate, "Fingertip Friction Modulation due to Electrostatic Attraction", *2013 World Haptics Conference (WHC)*, pp. 43–48, April 2013.

40. Nara, T., M. Takasaki, T. Maeda, T. Higuchi, S. Ando and S. Tachi, "Surface Acoustic Wave Tactile Display", *IEEE Computer Graphics and Applications*, Vol. 21, No. 6, pp. 56–63, 2001.

41. Winfield, L., J. Glassmire, J. E. Colgate and M. Peshkin, "T-PaD: Tactile Pattern Display through Variable Friction Reduction", *Second Joint EuroHaptics Conference and Symposium on Haptic Interfaces for Virtual Environment and Teleoperator Systems (WHC'07)*, pp. 421–426, IEEE, March 2007.

42. Biet, M., F. Giraud and B. Lemaire-Semail, "Implementation of Tactile Feedback by Modifying the Perceived Friction", *The European Physical Journal Applied Physics*, Vol. 43, No. 1, pp. 123–135, July 2008.

43. Strong, R. and D. Troxel, "An Electrotactile Display", *IEEE Transactions on Man Machine Systems*, Vol. 11, No. 1, pp. 72–79, March 1970.

44. Linjama, J. and V. Makinen, "E-Sense screen: Novel Haptic Display with Capac-

itive Electrosensory Interface", *HAID 2009, 4th Workshop for Haptic and Audio Interaction Design,*, 2009.

45. Harrison, C., "Quantifying the Targeting Performance Benefit of Electrostatic Haptic Feedback on Touchscreens", *ACM International Conference on Interactive Tabletops and Surfaces*, pp. 43–46, 2015.

46. Ghenna, S. and E. Vezzoli, "Friction Modulation by Ultrasonic Travelling Wave", *Journées des Jeunes Chercheurs en Génie Électrique*, Cherbourg, France, June 2015.

47. Watanabe, T. and S. Fukui, "A method for controlling tactile sensation of surface roughness using ultrasonic vibration", *Robotics and Automation, 1995. Proceedings., 1995 IEEE International Conference on*, Vol. 1, pp. 1134–1139, IEEE, 1995.

48. Biet, M., F. Giraud and B. Lemaire-Semail, "Implementation of tactile feedback by modifying the perceived friction", *The European Physical Journal-Applied Physics*, Vol. 43, No. 1, pp. 123–135, 2008.

49. Winfield, L., J. Glassmire, J. E. Colgate and M. Peshkin, "T-pad: Tactile pattern display through variable friction reduction", *EuroHaptics Conference, 2007 and Symposium on Haptic Interfaces for Virtual Environment and Teleoperator Systems. World Haptics 2007. Second Joint*, pp. 421–426, IEEE, 2007.

50. Marchuk, N. D., J. E. Colgate and M. A. Peshkin, "Friction measurements on a large area TPaD", *Haptics Symposium, 2010 IEEE*, pp. 317–320, IEEE, 2010.

51. Samur, E., J. E. Colgate and M. A. Peshkin, "Psychophysical evaluation of a variable friction tactile interface", Vol. 7240, p. 72400J, February 2009.

52. Chubb, E. C., J. E. Colgate and M. A. Peshkin, "ShiverPad: A device capable of controlling shear force on a bare finger", *EuroHaptics conference, 2009 and Symposium on Haptic Interfaces for Virtual Environment and Teleoperator Systems.*

World Haptics 2009. Third Joint, pp. 18–23, IEEE, 2009.

53. Dai, X., J. E. Colgate and M. A. Peshkin, "LateralPaD: A surface-haptic device that produces lateral forces on a bare finger", *Haptics Symposium (HAPTICS), 2012 IEEE*, pp. 7–14, IEEE, 2012.

54. Mullenbach, J., D. Johnson, J. E. Colgate and M. A. Peshkin, "ActivePaD surface haptic device", *Haptics Symposium (HAPTICS), 2012 IEEE*, pp. 407–414, IEEE, 2012.

55. Kim, J., K. J. Son and K. Kim, "An empirical study of rendering sinusoidal textures on a ultrasonic variable-friction haptic surface", *Ubiquitous Robots and Ambient Intelligence (URAI), 2015 12th International Conference on*, pp. 593–596, IEEE, 2015.

56. Messaoud, W. B., E. Vezzoli, F. Giraud and B. Lemaire-Semail, "Pressure dependence of friction modulation in ultrasonic devices", *World Haptic Conference*, 2015.

57. Friesen, R. F., M. Wiertlewski, M. A. Peshkin and J. E. Colgate, "The contribution of air to ultrasonic friction reduction", *World Haptics Conference (WHC), 2017 IEEE*, pp. 517–522, IEEE, 2017.

58. Wiertlewski, M., R. Fenton Friesen and J. E. Colgate, "Partial squeeze film levitation modulates fingertip friction.", *Proceedings of the National Academy of Sciences of the United States of America*, Vol. 113, No. 33, pp. 9210–9215, 2016.

59. Ghenna, S., F. Giraud, C. Giraud-Audine, M. Amberg and B. Lemaire-Semail, "Preliminary design of a multi-touch ultrasonic tactile stimulator", *IEEE World Haptics Conference, WHC 2015*, pp. 31–36, 2015.

60. Ghenna, S., C. Giraud-Audine, F. Giraud, M. Amberg and B. Lemaire-Semail, "Modal superimposition for multi-fingers variable friction tactile device", *Lec-*

ture Notes in Computer Science (including subseries Lecture Notes in Artificial Intelligence and Lecture Notes in Bioinformatics), Vol. 9774, pp. 521–530, 2016.

61. Marchuk, N. D., J. E. Colgate and M. A. Peshkin, "Friction measurements on a Large Area TPaD", *2010 IEEE Haptics Symposium*, pp. 317–320, IEEE, March 2010.

62. Meyer, D. J., M. Wiertlewski, M. A. Peshkin and J. E. Colgate, "Dynamics of ultrasonic and electrostatic friction modulation for rendering texture on haptic surfaces", *2014 IEEE Haptics Symposium (HAPTICS)*, pp. 63–67, February 2014.

63. Grimnes, S., "Electrovibration, Cutaneous Sensation of Microampere Current", *Acta Physiologica Scandinavica*, Vol. 118, No. 1, pp. 19–25, May 1983.

64. Mallinckrodt, E., A. L. Hughes and W. Sleator, "Perception by the Skin of Electrically Induced Vibrations", *Science*, Vol. 47, No. 4, pp. 277–278, 1953.

65. Israr, A. and S.-C. Kim, "Tactile Feedback on Flat Surfaces for the Visually Impaired", *ACM SIGCHI Conference on Human Factors in Computing Systems*, pp. 1571–1576, 2012.

66. Meyer, D. J., M. Wiertlewski, M. A. Peshkin and J. E. Colgate, "Dynamics of Ultrasonic and Electrostatic Friction Modulation for Rendering Texture on Haptic Surfaces", *2014 IEEE Haptics Symposium (HAPTICS)*, pp. 63–67, IEEE, February 2014.

67. Israr, A., O. Bau, S.-C. Kim and I. Poupyrev, "Tactile feedback on flat surfaces for the visually impaired", *CHI'12 Extended Abstracts on Human Factors in Computing Systems*, pp. 1571–1576, ACM, 2012.

68. Xu, C., A. Israr, I. Poupyrev, O. Bau and C. Harrison, "Tactile display for the visually impaired using TeslaTouch", *CHI'11 Extended Abstracts on Human Factors in Computing Systems*, pp. 317–322, ACM, 2011.

69. Osgouei, R. H., J. R. Kim and S. Choi, "Identification of primitive geometrical shapes rendered using electrostatic friction display", *IEEE Haptics Symposium, HAPTICS*, Vol. 2016-April, pp. 198–204, 2016.

70. Kim, H., J. Kang, K.-D. Kim, K.-M. Lim and J. Ryu, "Method for providing electrovibration with uniform intensity", *IEEE transactions on haptics*, Vol. 8, No. 4, pp. 492–496, 2015.

71. Basdogan, C., C. Ho and M. A. Srinivasan, "A raybased haptic rendering technique for displaying shape and texture of 3D objects in virtual environments", *ASME Winter Annual Meeting*, Vol. 61, pp. 77–84, 1997.

72. Wu, S., X. Sun, Q. Wang and J. Chen, "Tactile modeling and rendering image-textures based on electrovibration", *The Visual Computer*, Vol. 33, No. 5, pp. 637–646, 2017.

73. Wang, T. and X. Sun, "Electrostatic tactile rendering of image based on shape from shading", *2014 International Conference on Audio, Language and Image Processing*, pp. 775–779, IEEE, July 2014.

74. Vardar, Y., B. Guclu and C. Basdogan, "Effect of Waveform on Tactile Perception by Electrovibration Displayed on Touch Screens", *IEEE Transactions on Haptics*, Vol. 1412, No. c, pp. 1–1, 2017.

75. Kaczmarek, K. A., K. Nammi, A. K. Agarwal, M. E. Tyler, S. J. Haase and D. J. Beebe, "Polarity effect in electrovibration for tactile display.", *IEEE Transactions on Biomedical Engineering*, Vol. 53, No. 10, pp. 2047–2054, 2006.

76. Kang, J., S. Member, H. Kim, S. Member, S. Choi, K.-d. Kim, J. Ryu and A. Stimuli, "Preliminary Study on Perceived Intensity of Electrovibration Using High-Frequency Carrier-Signal Voltage", Vol. 12, 2015.

77. Kang, J., H. Kim, S. Choi, K.-D. Kim and J. Ryu, "Investigation on Low Voltage

Operation of Electrovibration Display", *IEEE Transactions on Haptics*, Vol. 1412, No. c, pp. 1–1, 2016.

78. Takazawa, K., A. Koike and Y. Ochiai, "Cross-Field Haptics : Push-Pull Haptics Combined with Magnetic and Electrostatic Fields", *ACM SIGGRAPH 2016 Posters*, 2016.

79. Pyo, D., S. Ryu, S.-C. Kim and D.-S. Kwon, "A new surface display for 3D haptic rendering", *International Conference on Human Haptic Sensing and Touch Enabled Computer Applications*, pp. 487–495, Springer, 2014.

80. Lee, J. U., J. M. Lim, H. Shin and K. U. Kyung, "A haptic touchscreen interface for mobile devices", *Proceedings of the 15th ACM on International conference on multimodal interaction - ICMI '13*, pp. 311–312, 2013.

81. Giraud, F., M. Amberg and B. Lemaire-Semail, "Merging two tactile stimulation principles: electrovibration and squeeze film effect", *2013 World Haptics Conference (WHC)*, pp. 199–203, IEEE, April 2013.

82. Vezzoli, E., W. B. Messaoud, M. Amberg, F. Giraud, B. Lemaire-Semail and M.-A. Bueno, "Physical and perceptual independence of ultrasonic vibration and electrovibration for friction modulation", *IEEE transactions on haptics*, Vol. 8, No. 2, pp. 235–239, 2015.

83. Wang, Q., X. Ren and X. Sun, "EV-pen: an electrovibration haptic feedback pen for touchscreens", *SIGGRAPH ASIA 2016 Emerging Technologies*, p. 8, ACM, 2016.

84. Nakamura, T. and A. Yamamoto, "A multi-user surface visuo-haptic display using electrostatic friction modulation and capacitive-type position sensing", *IEEE transactions on haptics*, Vol. 9, No. 3, pp. 311–322, 2016.

85. Nakamura, T. and A. Yamamoto, "Interaction force estimation on a built-in po-

sition sensor for an electrostatic visuo-haptic display", *ROBOMECH Journal*, Vol. 3, No. 1, p. 11, 2016.

86. Nakamura, T. and A. Yamamoto, "Position and force-direction detection for multi-finger electrostatic haptic system using a vision-based touch panel", *Proceedings of IARIA ACHI*, pp. 160–165, 2014.

87. Nakamura, T. and A. Yamamoto, "Multi-finger electrostatic passive haptic feedback on a visual display", *World Haptics Conference (WHC), 2013*, pp. 37–42, IEEE, 2013.

88. Shultz, C. D., M. A. Peshkin and J. E. Colgate, "Surface haptics via electroadhesion: Expanding electrovibration with Johnsen and Rahbek", *2015 IEEE World Haptics Conference (WHC)*, pp. 57–62, IEEE, June 2015.

89. Koh, K., M. Sreekumar and S. Ponnambalam, "Experimental Investigation of the Effect of the Driving Voltage of an Electroadhesion Actuator", *Materials*, Vol. 7, No. 7, pp. 4963–4981, 2014.

90. Mullenbach, J., M. Peshkin and J. E. Colgate, "eShiver: Force feedback on fingertips through oscillatory motion of an electroadhesive surface", *IEEE Haptics Symposium, HAPTICS*, Vol. 2016-April, No. X, pp. 271–276, 2016.

91. Alma, U. A., G. Ilkhani and E. Samur, "On Generation of Active Feedback with Electrostatic Attraction", *Lecture Notes in Computer Science (including subseries Lecture Notes in Artificial Intelligence and Lecture Notes in Bioinformatics)*, Vol. 9775, pp. 449–458, 2016.

92. Haga, H., K. Yoshinaga, J. Yanase, D. Sugimoto, K. Takatori and H. Asada, "Electrostatic Tactile Display Using Beat Phenomenon for Stimulus Localization", *IEICE Transactions on Electronics*, Vol. 98, No. 11, pp. 1008–1014, 2015.

93. Kim, K. D., Y. Choi, S. H. Yoon, J. Kang, H. Kim and J. Ryu, "An electrostatic

haptic display with a projected capacitive touch screen", *SID Symposium Digest of Technical Papers*, Vol. 47, No. 1, pp. 506–509, 2016.

94. Butikofer, R. and P. D. Lawrence, "Electrocutaneous nerve stimulation-I: Model and experiment", *IEEE Transactions on Biomedical Engineering*, , No. 6, pp. 526–531, 1978.

95. Kajimoto, H., Y. Kanno and S. Tachi, "Forehead electro-tactile display for vision substitution", *Proc. EuroHaptics*, 2006.

96. Kajimoto, H., M. Inami, N. Kawakami and S. Tachi, "Smarttouch-augmentation of skin sensation with electrocutaneous display", *Haptic Interfaces for Virtual Environment and Teleoperator Systems, 2003. HAPTICS 2003. Proceedings. 11th Symposium on*, pp. 40–46, IEEE, 2003.

97. Kajimoto, H., "Electrotactile display with real-time impedance feedback using pulse width modulation", *IEEE transactions on haptics*, Vol. 5, No. 2, pp. 184–188, 2012.

98. Kajimoto, H., N. Kawakami, T. Maeda and S. Tachi, "Tactile feeling display using functional electrical stimulation", *Proc. 1999 ICAT*, p. 133, 1999.

99. Echenique, A. and J. Graffigna, "Electrical stimulation of mechanoreceptors", *Journal of Physics: Conference Series*, Vol. 332, p. 012044, IOP Publishing, 2011.

100. Haase, S. J. and K. A. Kaczmarek, "Electrotactile perception of scatterplots on the fingertips and abdomen", *Medical and Biological Engineering and Computing*, Vol. 43, No. 2, pp. 283–289, 2005.

101. Bach-y Rita, P., K. A. Kaczmarek, M. E. Tyler and J. Garcia-Lara, "Form perception with a 49-point electrotactile stimulus array on the tongue: a technical note.", *Journal of rehabilitation research and development*, Vol. 35, No. 4, pp. 427–30, October 1998.

102. Higashiyama, A. and G. B. Rollman, "Perceived locus and intensity of electrocutaneous stimulation", *IEEE Transactions on Biomedical Engineering*, Vol. 38, No. 7, pp. 679–686, 1991.

103. Altinsoy, M. E. and S. Merchel, "Electrotactile Feedback for Handheld Devices with Touch Screen and Simulation of Roughness", *IEEE Transactions on Haptics*, Vol. 5, No. 1, pp. 6–13, January 2012.

104. Nikolovski, J.-P. and D. Fournier, "Lamb wave (X, Y) detector", *Electronics Letters*, Vol. 32, No. 12, pp. 1147–1148, 1996.

105. Ing, R. K., D. Cassereau, M. Fink and J.-P. Nikolovski, "Tactile touch plate with variable boundary conditions", *Journal of the Acoustical Society of America*, Vol. 123, No. 5, p. 3643, 2008.

106. Liu, Y., J. Nikolovski, N. Mechbal, M. Hafez and M. Vergé, "A Multi-Touch Plate Based on Lamb Wave Absorption", *Procedia Chemistry*, Vol. 1, No. 1, pp. 156–159, September 2009.

107. Hudin, C., J. Lozada and V. Hayward, "Localized tactile stimulation by time-reversal of flexural waves: Case study with a thin sheet of glass", *2013 World Haptics Conference (WHC)*, pp. 67–72, April 2013.

108. Hudin, C., M. Wiertlewski and V. Hayward, "Tradeoffs in the Application of Time-Reversed Acoustics to Tactile Stimulation", pp. 218–226, 2012.

109. Ikei, Y. and M. Yamada, "Tactile Texture Presentation by Vibratory Pin-Arrays based on Surface Height-maps", *Transactions of the Virtual Reality Society of Japan*, Vol. 7, No. 2, pp. 247–255, 2002.

110. Hayward, V. and M. Cruz-Hernandez, "Tactile display device using distributed lateral skin stretch", *Proceedings of the haptic interfaces for virtual environment and teleoperator systems symposium*, Vol. 69, pp. 1309–1314, ASME, 2000.

111. Pasquero, J. and V. Hayward, "STRESS: A practical tactile display system with one millimeter spatial resolution and 700 Hz refresh rate", *Proc. of Eurohaptics 2003*, pp. 94–110, 01 2003.

112. Romano, J. M. and K. J. Kuchenbecker, "Creating Realistic Virtual Textures from Contact Acceleration Data", *IEEE Transactions on Haptics*, Vol. 5, No. 2, pp. 109–119, April 2012.

113. Culbertson, H., J. Unwin and K. J. Kuchenbecker, "Modeling and Rendering Realistic Textures from Unconstrained Tool-Surface Interactions", *IEEE Transactions on Haptics*, Vol. 7, No. 3, pp. 381–393, July 2014.

114. Saga, S. and R. Raskar, "Simultaneous Geometry and Texture Display Based on Lateral Force for Touchscreen", *2013 World Haptics Conference (WHC)*, pp. 437–442, IEEE, April 2013.

115. Yamamoto, A., S. Nagasawa, H. Yamamoto and T. Higuchi, "Electrostatic tactile display with thin film slider and its application to tactile telepresentation systems", *IEEE Transactions on Visualization and Computer Graphics*, Vol. 12, No. 2, pp. 168–177, March 2006.

116. Höver, R., M. Harders and G. Székely, "Data-driven Haptic Rendering of Visco-elastic Effects", *Symposium on Haptics Interfaces for Virtual Environment and Teleoperator Systems 2008 - Proceedings, Haptics*, pp. 201–208, 2008.

117. Höver, R., G. Kósa, G. Székely and M. Harders, "Data-driven Haptic Rendering - From Viscous Fluids to Visco-Elastic Solids", *IEEE Transactions on Haptics*, Vol. 2, No. 1, pp. 15–27, 2009.

118. Agarwal, A., K. Nammi, K. Kaczmarek, M. Tyler and D. Beebe, "A hybrid natural/artificial electrostatic actuator for tactile stimulation", *2nd Annual International IEEE-EMBS Special Topic Conference on Microtechnologies in Medicine and Biology.*, Vol. 1, pp. 341–345, IEEE, Madison, WI, 2002.

119. Hui Tang and D. Beebe, "A microfabricated electrostatic haptic display for persons with visual impairments", *IEEE Transactions on Rehabilitation Engineering*, Vol. 6, No. 3, pp. 241–248, 1998.

120. Smythe, W. R. W. R., *Static and dynamic electricity*, McGraw-Hill, New York; London, 2nd ed. edn., 1950.

121. Ilkhani, G., M. Aziziaghdam and E. Samur, "Data-Driven Texture Rendering on an Electrostatic Tactile Display", *International Journal of Human–Computer Interaction*, Vol. 00, No. 00, pp. 1–15, 2017.

122. Konyo, M., S. Tadokoro, A. Yoshida and N. Saiwaki, "A Tactile Synthesis Method Using Multiple Frequency Vibrations for Representing Virtual Touch", *2005 IEEE/RSJ International Conference on Intelligent Robots and Systems*, pp. 3965–3971, 2005.

123. Wiertlewski, M., J. Lozada and V. Hayward, "The Spatial Spectrum of Tangential Skin Displacement Can Encode Tactual Texture", *IEEE Transactions on Robotics*, Vol. 27, No. 3, pp. 461–472, June 2011.

124. Culbertson, H., J. J. L. Delgado and K. J. Kuchenbecker, "One Hundred Data-driven Haptic Texture Models and Open-source Methods for Rendering on 3D Objects", *2014 IEEE Haptics Symposium (HAPTICS)*, pp. 319–325, IEEE, February 2014.

125. Cornsweet, T. N., "The Staircase-Method in Psychophysics", *The American Journal of Psychology*, Vol. 75, No. 3, p. 485, September 1962.

126. Leskovsky, P., T. Cooke, M. Ernst and M. Harders, "Using Multidimensional Scaling to Quantify the Fidelity of Haptic Rendering of Deformable Objects", *EuroHaptics 2006 International Conference*, pp. 289–295, paris, 2006.

127. Preston, C. C. and A. M. Colman, "Optimal Number of Response Categories

in Rating Scales: Reliability, Validity, Discriminating Power, and Respondent Preferences.", *Acta psychologica*, Vol. 104, No. 1, pp. 1–15, 2000.

128. Lederman, S. J. and R. L. Klatzky, "Hand movements: A window into haptic object recognition", *Cognitive Psychology*, Vol. 19, No. 3, pp. 342–368, July 1987.

129. Johnson, K. O., S. S. Hsiao and T. Yoshioka, "Neural coding and the basic law of psychophysics", *The Neuroscientist*, Vol. 8, No. 2, pp. 111–121, 2002.

130. Connor, C. E. and K. O. Johnson, "Neural coding of tactile texture: comparison of spatial and temporal mechanisms for roughness perception.", *The Journal of neuroscience : the official journal of the Society for Neuroscience*, Vol. 12, No. 9, pp. 3414–26, September 1992.

131. Guruswamy, V. L., J. Lang and W.-S. Lee, "IIR Filter Models of Haptic Vibration Textures", *IEEE Transactions on Instrumentation and Measurement*, Vol. 60, No. 1, pp. 93–103, January 2011.

132. Culbertson, H. and K. J. Kuchenbecker, "Should haptic texture vibrations respond to user force and speed?", *2015 IEEE World Haptics Conference (WHC)*, pp. 106–112, IEEE, June 2015.

133. Vezzoli, E., M. Amberg, F. Giraud and B. Lemaire-Semail, "Electrovibration Modeling Analysis", M. Auvray and C. Duriez (Editors), *Haptics: Neuroscience, Devices, Modeling, and Applications Lecture Notes in Computer Science*, pp. 369–376, Springer Berlin Heidelberg, 2014.

134. Yoshioka, T., B. Gibb, A. K. Dorsch, S. S. Hsiao and K. O. Johnson, "Neural coding mechanisms underlying perceived roughness of finely textured surfaces.", *The Journal of neuroscience : the official journal of the Society for Neuroscience*, Vol. 21, No. 17, pp. 6905–16, September 2001.

135. Weber, A. I., H. P. Saal, J. D. Lieber, J.-W. Cheng, L. R. Manfredi, J. F.

Dammann and S. J. Bensmaia, "Spatial and temporal codes mediate the tactile perception of natural textures.", *Proceedings of the National Academy of Sciences of the United States of America*, Vol. 110, No. 42, pp. 17107–12, 2013.

136. Haga, H., K. Yoshinaga, J. Yanase, D. Sugimoto, K. Takatori and H. Asada, "Electrostatic Tactile Display Using Beat Phenomenon for Stimulus Localization", *IEICE Transactions on Electronics*, Vol. 98, No. 11, pp. 1008–1014, 2015.

137. Kim, S., W. Choi, W. Rim, Y. Chun, H. Shim, H. Kwon, J. Kim, I. Kee, S. Kim, S. Lee and J. Park, "A Highly Sensitive Capacitive Touch Sensor Integrated on a Thin-Film-Encapsulated Active-Matrix OLED for Ultrathin Displays", *IEEE Transactions on Electron Devices*, Vol. 58, No. 10, pp. 3609–3615, October 2011.

138. ilkhani, G., M. Aziziaghdam and E. Samur, "Creating Localized Haptic Feedback on A Tactile Display Using Electrostatic Attraction", *World Haptics Conference (WHC), Work in Progress*, IEEE, 2015.

139. Vardar, Y., B. Guclu and C. Basdogan, "Effect of Waveform on Tactile Perception by Electrovibration Displayed on Touch Screens", *IEEE Transactions on Haptics*, Vol. PP, No. 99, pp. 1–1, 2017.

140. Samur, E., *Performance metrics for haptic interfaces*, Springer Science & Business Media, 2012.

141. Ilkhani, G., M. Aziziaghdam and E. Samur, "Data-driven texture rendering with electrostatic attraction", *International Conference on Human Haptic Sensing and Touch Enabled Computer Applications*, pp. 496–504, Springer, 2014.

142. Ilkhani, G., M. Aziziaghdam and E. Samur, "Creating Localized Haptic Feedback on a Tactile Display Using Electrostatic Attraction", *World Haptic Conference-Work in Progress*, IEEE, 2015.

143. Ilkhani, G., M. Aziziaghdam and E. Samur, "Data-Driven Texture Rendering

on an Electrostatic Tactile Display", *International Journal of Human–Computer Interaction*, Vol. 33, No. 9, pp. 756–770, 2017.

144. "A Touch Sensor Controller IC Adopting Differential Measurement for Projected Capacitive Touch Panel Systems", *2012 IEEE 12th International Conference on Computer and Information Technology*, pp. 477–481, IEEE, October 2012.

145. Walker, G., "Fundamentals of touch technologies and applications", *Society for Information Display*, 2011.

APPENDIX A: TOUCH SENSORS

There are different types of tactile sensors available with different mechanical and electrical characteristics. Major commercialized touch screens use acoustic-wave, infrared, resistive, and capacitive sensing methods [144]. Among all these products the analogue resistive, surface capacitive, and projected capacitive touch sensors are dominant.

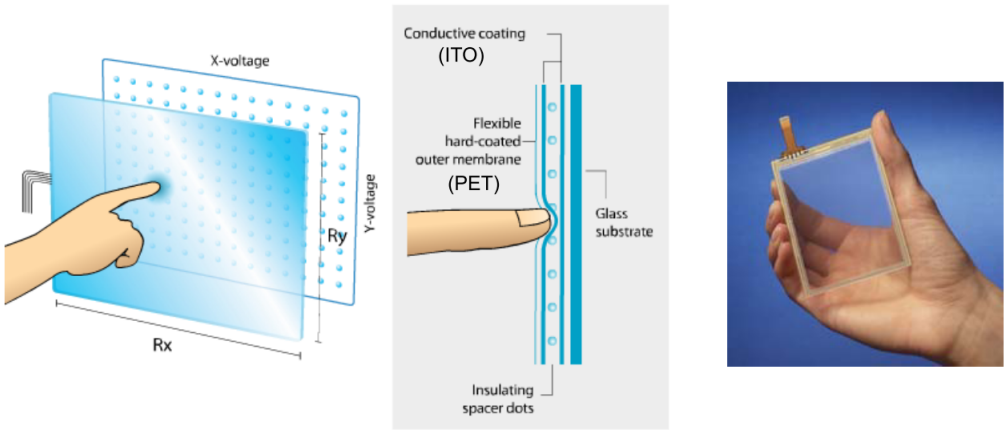

Figure A.1. Resistive touch sensor is the simplest type of touch technology to find the finger position. Detecting parameter in this technology is the varying resistance between two conductive surface [145].

A.1. Analogue Resistive

Analogue resistive is classified as transparent, continues the type of touch display composed of two layers of ITO separated from each other with tiny separators. When a finger touches the surface, resistance changes between two ITO layers and thus touches location is determined. The measurement parameter in this type of display is the voltage. A multi-touch type known as MARS (Multi-touch Analogue Resistive Sensor) is more or less same structure in distributed format. The problem happens if you push the same region with two fingers [137].

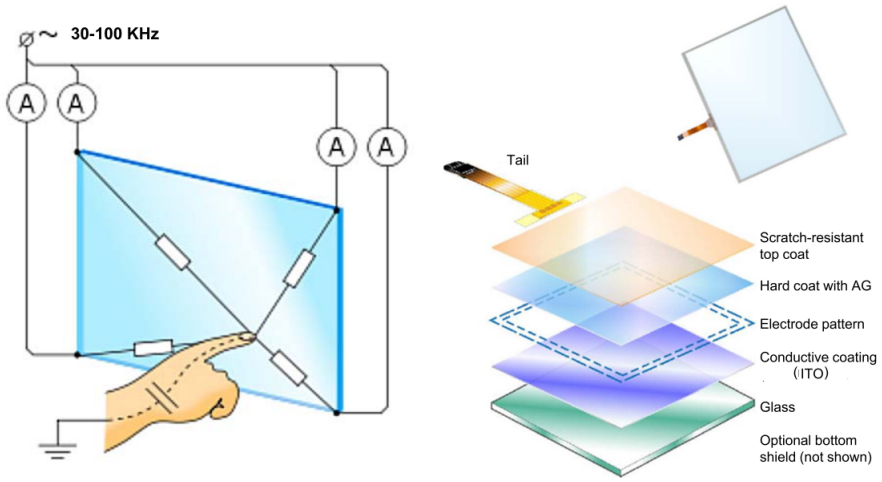

Figure A.2. The most known example of capacitive sensing technology is 3M micro touch panel as described in chapter 3. Current is measured to detect finger position [145].

A.2. Surface Capacitive

Surface capacitive is normally used as a single touch, transparent touch sensor. The surface capacitive sensor is constructed of three main layers: a glass substrate, ITO coating and a hard coat of SiO2 (Silica) at the top. Current is measured to find the finger position [137]. Since its principal of detection is capacitive, it is suitable to employ the electrovibration phenomenon. Several research groups use this type of sensor to create different artificial textures. 3M MicroTouch is the well-known screen among the haptic community and used frequently for surface haptics.

A.3. Projected Capacitive Touch Sensor

Projected capacitive touch sensor, known as P-Cap, is the transparent and patterned type of multi-touch sensor. Typically, it is composed of interlocking diamond shape electrode lines. The horizontal X (signal line) and vertical Y (sense line) rout of conductive electrodes uniformly distributed on the surface. Finger position is determined based on a change in capacitance of sense line (self-capacitance) plus the change in capacitance with respect to other sense line (mutual-capacitance) [137]. In order to

reach a high resolution and good performance, P-Cap can be found in different structures such as G1F (sensor film with ITO laminated to the glass on one side), GFF (two sensor films laminated to glass), SITO (single sided ITO on glass). In SITO, drive and sense electrodes are on a single ITO layer where the Y line electrodes are bridged at the intersection with the X line electrodes (Figure A.3). The optically clear adhesive (OCA) binds layers and a protective film is often the upmost layer.

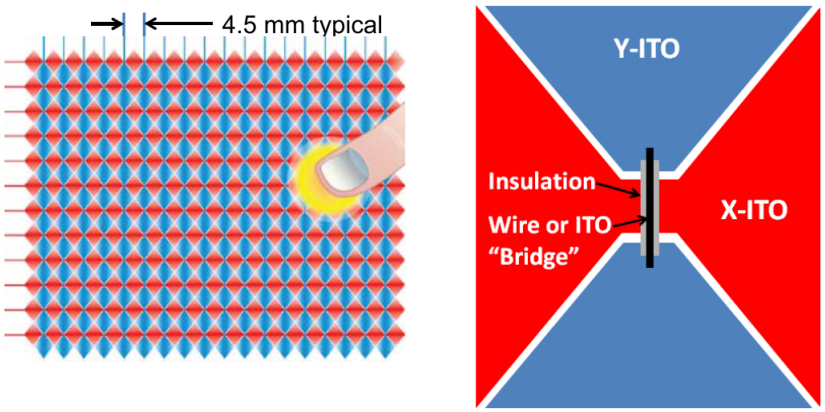

Figure A.3. P-Cap is found in different configurations. Detection parameter in this technology is capacitance variation due to mutual capacitance and self capacitance [145].